

vectors into diseased muscle, this system seemed to be useful in modifying genetically autologous cells *ex vivo* rather than in direct injection *in vivo*. In fact, lentiviral vectors expressing mini-dystrophin transduced mouse satellite cells efficiently, and the transduced cells regenerated muscle fibers after transplantation [28]. Quenneville et al. [29] showed that lentiviral vectors are useful in transducing monkey muscle stem cells. The lentiviral vector has been recently used to modify muscle stem cells to deliver an antisense sequence linked to a modified U7 [30] or U1 [31] small nuclear RNA for restoration of the reading frame.

Antisense oligonucleotide (AO)-mediated exon skipping for DMD gene

Skipping of targeted exons

DMD is caused by mutations in the *DMD* gene that disrupt the open reading frame. BMD is also caused by mutations in the *DMD* gene, but in the case of BMD, the open reading frame is maintained. If we can skip (splice out) targeted exons by modification of splicing patterns and restore the reading frame, a shorter dystrophin protein can be restored in the DMD muscle, converting the DMD phenotype to a BMD phenotype. To this end, a number of antisense oligonucleotides (AOs) have been designed and tested *in vitro* [32–34] and *in vivo* [35–37]. Fig. 1 illustrates the skipping of exon 51 using one AO. Whether the resultant shortened dystrophin is functional or not depends largely on the function of the deleted part. In general, truncation of the rod domain is thought to be relatively harmless.

Single exon 51 skipping is expected to be suitable for approximately 13% of DMD patients. Multiple exon skipping is estimated to be applicable to more than 80% of DMD patients. Theoretically, the AO-mediated exon skipping strategy cannot treat patients with mutations in the promoter region, deletion of the first or last (79th)

exon, deletion of the domain bound by dystroglycan: exons 62–69 [38] or large deletions (>35 exons) [39]. However, these mutations are rare, and the majority of patients have a mutation in the hotspot located between exons 43 and 55.

Design of AOs

AOs are designed to hybridize specific sequences, such as exon-intron boundaries, and exon splicing enhancer (ESE) sequences in transcripts. AOs interfere sterically with the splicing machinery [40,41]. There are several software programs, such as ESEfinder (<http://rulai.cshl.edu/tools/ESE>), to design antisense oligonucleotides, but extensive empirical analysis is still required for each exon.

AO chemistry, delivery *in vivo*, and toxicity

Among the AOs tested so far, AOs having a 2'-O-methyl phosphorothioate backbone (2'-O-MeAO) and phosphorodiamidate morpholino oligomers (PMOs) (Fig. 2) are commonly used in animal models and in clinical trials [42,43]. 2'-O-MeAOs have a chemically modified RNA structure (Fig. 2). The modifications increase the half-life and distribution to tissues. 2'-O-MeAOs have been well tolerated in clinical trials. PMOs have a morpholino backbone, are uncharged, are not recognized by cellular proteins, and, therefore, are rapidly cleared from plasma and excreted in urine. Very high doses of PMOs are reported to be well tolerated by animal models. This would be partly because PMOs hardly evoke innate immune responses.

In vivo delivery of AOs

One limitation of PMO-mediated exon-skipping therapy is that PMOs do not easily enter cardiac muscle. Recently, to improve the uptake of PMOs by cardiocytes, peptide-tagged PMOs (PPMOs) [44] and Octa-guanidine PMOs [45] were developed. These modified

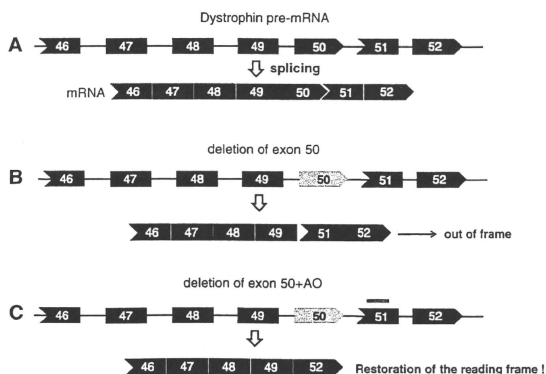


Fig. 1 – Exon skipping therapy for DMD patients with deletion of exon 51. (A) Normal dystrophin transcript and mRNA. (B) Deletion of exon 50 disrupts the open reading frame, leading to a premature stop codon, unstable mRNA, and a truncated protein. (C) Targeted skipping of exon 51 using AO restores the reading frame and produces a shorter but functional dystrophin that lacks exons 50 and 51. Blue bar indicates AO targeting the sequence in exon 51.

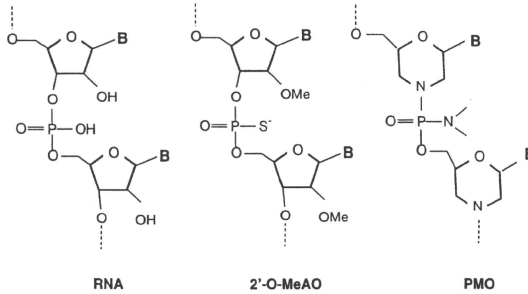


Fig. 2 – Structure of RNA, 2'-O-MeAO, and PMO. B: bases (adenine, cytosine, guanine, and thymine).

morpholinos are reported to be more effective than native PMOs in inducing exon skipping in cardiac muscle after intravascular injection. But there are potential concerns that PPMOs might elicit an immune response or have toxicity compared with PMOs due to the protein moiety.

Skipping multiple exons

If fully approved, AVI-4658 and PRO051, both of which target dystrophin exon 51, will be able to treat 13% of DMD patients. To treat more patients, elimination of two or more exons from the final mRNA is required. Theoretically, multiexon skipping using a cocktail of AOs can restore the reading frame of the *DMD* gene in more than 83% of the all DMD patients. Double-exon skipping using AOs has been shown to be feasible in patient-derived cells [46], mouse models, and dystrophic dogs [37]. On the other hand, the efficiency of multiexon skipping is much lower than expected [47]. This is presumably because partial exon skipping results in out-of-frame transcripts. It will be some time before multiple-exon skipping is applied to DMD patients.

Ongoing clinical trials of exon skipping

Clinical trials using intramuscular administration of 51 AOs, PRO051 (2'-O-Me AO), and AVI-4658 (PMO) have been performed in Europe by Prosenza and AVI BioPharma respectively. PRO051 and AVI-4658 were both designed to induce exon 51 skipping in the *DMD* gene and, therefore, can treat DMD patients with deletions such as 45–50, 47–50, 48–50, 49–50, 50, or 52. AVI BioPharma reported the initial data of systemic treatment with AVI-4658 (a phase 1b/2 clinical study) in the United Kingdom, which resulted in the successful restoration of dystrophin in the 2-mg/kg dose cohort (<http://www.avibio.com/>). AVI-4658 is well tolerated and so far has caused no serious side effects in treated patients. A phase 1/2 dose-ranging safety study using PRO051 was performed on 12 patients at two European clinical centers. The study demonstrated that PRO051 was also well tolerated up to 6 mg/kg and that novel dystrophin expression was detected in the patients in response to injections above 0.5 mg/kg [48] (also refer to <http://prosenza.eu/technology-and-products/Pipeline/PRO-051.php> or http://www.parentproject.org.au/html/s02_article/view.asp?art_id=6798&nav_catid=2148&nav_top_id=78).

However, the consequences of long-term administration of both AOs should be carefully examined because AOs have a transient effect and must be readministered to sustain the effect.

Conclusions

Development of gene therapy for DMD has long been a challenge, but recent strategies, such as AAV-8 or AAV-9-mediated systemic delivery of microdystrophin and exon skipping, hold great potential. AO-induced exon skipping is a mutation-specific approach. Both the mutation and splicing patterns of dystrophin mRNA must be examined individually, and the AO sequences used would differ from patient to patient. One concern is that the efficacy and safety of each variation must be tested on the same backbone, requiring more time to get approval from the regulatory authorities.

Although AO-mediated exon skipping has shown promising results, the authors predict that a combination of exon skipping and other therapeutic approaches, such as viral vector-mediated gene transfer, stem cell-based therapy, or additional strategies of enhancing muscle regeneration, will become the standard approach for future DMD therapy.

Acknowledgments

We would like to thank all members of the laboratory for helpful discussions.

REFERENCES¹

- [1] A. Aartsma-Rus, J.C. Van Deutekom, I.F. Fokkema, G.J. Van Ommen, J.T. Den Dunnen, Entries in the Leiden Duchenne muscular dystrophy mutation database: an overview of mutation types and paradoxical cases that confirm the reading-frame rule, *Muscle Nerve* 34 (2006) 135–144.

¹ The authors apologize that due to the limitation of space, all relevant references are not cited.

- [2] K.P. Campbell, Three muscular dystrophies: loss of cytoskeleton–extracellular matrix linkage, *Cell* 80 (1995) 675–679.
- [3] G. Gao, L.H. Vandenbergh, J.M. Wilson, New recombinant serotypes of AAV vectors, *Curr. Gene Ther.* 5 (2005) 285–297.
- [4] C. Trollet, T. Athanasopoulos, L. Poppelwell, A. Malerba, G. Dickson, Gene therapy for muscular dystrophy: current progress and future prospects, *Expert Opin. Biol. Ther.* 9 (2009) 849–866.
- [5] A.L. Arnett, J.R. Chamberlain, J.S. Chamberlain, Therapy for neuromuscular disorders, *Curr. Opin. Genet. Dev.* 19 (2009) 290–297.
- [6] K. Foster, H. Foster, J.G. Dickson, Gene therapy progress and prospects: Duchenne muscular dystrophy, *Gene Ther.* 13 (2006) 1677–1685.
- [7] P. Gregorevic, M.J. Blankinship, J.M. Allen, R.W. Crawford, L. Meuse, D.G. Miller, D.W. Russell, J.S. Chamberlain, Systemic delivery of genes to striated muscles using adeno-associated viral vectors, *Nat. Med.* 10 (2004) 828–834.
- [8] A. Nishiyama, B.N. Ampong, S. Ohshima, J.H. Shin, H. Nakai, M. Imamura, Y. Miyagoe-Suzuki, T. Okada, S. Takeda, Recombinant adeno-associated virus type 8-mediated extensive therapeutic gene delivery into skeletal muscle of alpha-sarcoglycan-deficient mice, *Hum. Gene Ther.* 19 (2008) 719–730.
- [9] Z. Wang, T. Zhu, C. Qiao, L. Zhou, B. Wang, J. Zhang, C. Chen, J. Li, X. Xiao, Adeno-associated virus serotype 8 efficiently delivers genes to muscle and heart, *Nat. Biotechnol.* 23 (2005) 321–328.
- [10] K. Inagaki, S. Fuess, T.A. Storm, G.A. Gibson, C.F. McTiernan, M.A. Kay, H. Nakai, Robust systemic transduction with AAV9 vectors in mice: efficient global cardiac gene transfer superior to that of AAV8, *Mol. Ther.* 14 (2006) 45–53.
- [11] L.T. Bish, K. Morine, M.M. Sleeper, J. Sanmiguel, D. Wu, G. Gao, J.M. Wilson, H.L. Sweeney, Adeno-associated virus (AAV) serotype 9 provides global cardiac gene transfer superior to AAV1, AAV6, AAV7, and AAV8 in the mouse and rat, *Hum. Gene Ther.* 19 (2008) 1359–1368.
- [12] C.A. Pacak, C.S. Mah, B.D. Thattaliyath, T.J. Conlon, M.A. Lewis, D.E. Cloutier, I. Zolotukhin, A.F. Tarantali, B.J. Byrne, Recombinant adeno-associated virus serotype 9 leads to preferential cardiac transduction in vivo, *Circ. Res.* 99 (2006) e3–e9.
- [13] M. Yoshimura, M. Sakamoto, M. Ikemoto, Y. Mochizuki, K. Yuasa, Y. Miyagoe-Suzuki, S. Takeda, AAV vector-mediated microdystrophin expression in a relatively small percentage of mdx myofibers improved the mdx phenotype, *Mol. Ther.* 10 (2004) 821–828.
- [14] P. Gregorevic, M.J. Blankinship, J.M. Allen, J.S. Chamberlain, Systemic microdystrophin gene delivery improves skeletal muscle structure and function in old dystrophic mdx mice, *Mol. Ther.* 16 (2008) 657–664.
- [15] P. Gregorevic, J.M. Allen, E. Minami, M.J. Blankinship, M. Haraguchi, L. Meuse, E. Finn, M.E. Adams, S.C. Froehner, C.E. Murry, J.S. Chamberlain, rAAV6-microdystrophin preserves muscle function and extends lifespan in severely dystrophic mice, *Nat. Med.* 12 (2006) 787–789.
- [16] D. Townsend, M.J. Blankinship, J.M. Allen, P. Gregorevic, J.S. Chamberlain, J.M. Metzger, Systemic administration of micro-dystrophin restores cardiac geometry and prevents dobutamine-induced cardiac pump failure, *Mol. Ther.* 15 (2007) 1086–1092.
- [17] A. Ghosh, Y. Yue, Y. Lai, D. Duan, A hybrid vector system expands adeno-associated viral vector packaging capacity in a transgene-independent manner, *Mol. Ther.* 16 (2008) 124–130.
- [18] K. Yuasa, M. Yoshimura, N. Urasawa, S. Ohshima, J.M. Howell, A. Nakamura, T. Hijikata, Y. Miyagoe-Suzuki, S. Takeda, Injection of a recombinant AAV serotype 2 into canine skeletal muscles evokes strong immune responses against transgene products, *Gene Ther.* 14 (2007) 1249–1260.
- [19] S. Ohshima, J.H. Shin, K. Yuasa, A. Nishiyama, J. Kira, T. Okada, S. Takeda, Transduction efficiency and immune response associated with the administration of AAV8 vector into dog skeletal muscle, *Mol. Ther.* 17 (2009) 73–80.
- [20] L.R. Rodino-Klapac, P.M. Janssen, C.L. Montgomery, B.D. Coley, L.G. Chicoine, K.R. Clark, J.R. Mendell, A translational approach for limb vascular delivery of the micro-dystrophin gene without high volume or high pressure for treatment of Duchenne muscular dystrophy, *J. Transl. Med.* 5 (2007) 45.
- [21] L.R. Rodino-Klapac, C.L. Montgomery, W.G. Bremer, K.M. Shontz, V. Malik, N. Davis, S. Sprinkle, K.J. Campbell, Z. Sahenk, K.R. Clark, C.M. Walker, J.R. Mendell, L.G. Chicoine, Persistent expression of FLAG-tagged micro dystrophin in nonhuman primates following intramuscular and vascular delivery, *Mol. Ther.* 18 (2010) 109–117.
- [22] Z. Wang, J.M. Allen, S.R. Riddell, P. Gregorevic, R. Storb, S.J. Tapscott, J.S. Chamberlain, C.S. Kuhr, Immunity to adeno-associated virus-mediated gene transfer in a random-bred canine model of Duchenne muscular dystrophy, *Hum. Gene Ther.* 18 (2007) 18–26.
- [23] Z. Wang, C.S. Kuhr, J.M. Allen, M. Blankinship, P. Gregorevic, J.S. Chamberlain, S.J. Tapscott, R. Storb, Sustained AAV-mediated dystrophin expression in a canine model of Duchenne muscular dystrophy with a brief course of immunosuppression, *Mol. Ther.* 15 (2007) 1160–1166.
- [24] M.Z. Salva, C.L. Himeida, P.W. Tai, E. Nishiuchi, P. Gregorevic, J.M. Allen, E.E. Finn, Q.G. Nguyen, M.J. Blankinship, L. Meuse, J.S. Chamberlain, S.D. Hauschka, Design of tissue-specific regulatory cassettes for high-level RAAV-mediated expression in skeletal and cardiac muscle, *Mol. Ther.* 15 (2007) 320–329.
- [25] B. Wang, J. Li, F.H. Fu, C. Chen, X. Zhu, L. Zhou, X. Jiang, X. Xiao, Construction and analysis of compact muscle-specific promoters for AAV vectors, *Gene Ther.* 15 (2008) 1489–1499.
- [26] H. Foster, P.S. Sharp, T. Athanasopoulos, C. Trollet, I.R. Graham, K. Foster, D.J. Wells, G. Dickson, Codon and mRNA sequence optimization of microdystrophin transgenes improves expression and physiological outcome in dystrophic mdx mice following AAV2/8 gene transfer, *Mol. Ther.* 16 (2008) 1825–1832.
- [27] S. Li, E. Kimura, B.M. Fall, M. Reyes, J.C. Angello, R. Welikson, S.D. Hauschka, J.S. Chamberlain, Stable transduction of myogenic cells with lentiviral vectors expressing a microdystrophin, *Gene Ther.* 12 (2005) 1099–1108.
- [28] M. Ikemoto, S. Fukada, A. Uezumi, S. Masuda, H. Miyoshi, H. Yamamoto, M.R. Wada, N. Masubuchi, Y. Miyagoe-Suzuki, S. Takeda, Autologous transplantation of SM/C-2.6(+) satellite cells transduced with micro-dystrophin CSI cDNA by lentiviral vector into mdx mice, *Mol. Ther.* 15 (2007) 2178–2185.
- [29] S.P. Quenneville, P. Chappelaine, D. Skuk, M. Paradis, M. Goulet, J. Rousseau, X. Xiao, L. Garcia, J.P. Tremblay, Autologous transplantation of muscle precursor cells modified with a lentivirus for muscular dystrophy: human cells and primate models, *Mol. Ther.* 15 (2007) 431–438.
- [30] A. Goyenvallat, A. Vulin, F. Fougereuse, F. Leturcq, J.C. Kaplan, L. Garcia, D. Danos, Rescue of dystrophic muscle through U7 snRNA-mediated exon skipping, *Science* 306 (2004) 1796–1799.
- [31] M.A. Denti, A. Rosa, G. D'Antona, O. Stanchieri, F.G. De Angelis, C. Nicoletti, M. Allocca, O. Pansarasa, V. Parente, A. Musaro, A. Auricchio, R. Bottinelli, I. Bozzoni, Body-wide gene therapy of Duchenne muscular dystrophy in the mdx mouse model, *Proc Natl Acad Sci U S A* 103 (2006) 3758–3763.
- [32] S.D. Wilton, A.M. Fall, P.L. Harding, G. McCloy, C. Coleman, S. Fletcher, Antisense oligonucleotide-induced exon skipping across the human dystrophin gene transcript, *Mol. Ther.* 15 (2007) 1288–1296.
- [33] A. Aartsma-Rus, L. van Vliet, M. Hirschi, A.A. Janson, H. Heemskerk, C.L. de Winter, S. de Kimpfe, J.C. van Deutekom, P.A. t Hoen, G.J. van Ommen, Guidelines for antisense oligonucleotide design and insight into splice-modulating mechanisms, *Mol. Ther.* 17 (2009) 548–553.
- [34] L.J. Poppelwell, C. Adkin, V. Arechavala-Gomez, A. Aartsma-Rus, C.L. de Winter, S.D. Wilton, J.E. Morgan, F. Muntoni, I.R. Graham, G. Dickson, Comparative analysis of antisense oligonucleotide sequences targeting exon 53 of the human DMD gene:

- implications for future clinical trials, *Neuromuscul. Disord.* 20 (2010) 102–110.
- [35] Q.L. Lu, C.J. Mann, F. Lou, G. Bou-Gharios, G.E. Morris, S.A. Xue, S. Fletcher, T.A. Partridge, S.D. Wilton, Functional amounts of dystrophin produced by skipping the mutated exon in the mdx dystrophic mouse, *Nat. Med.* 9 (2003) 1009–1014.
- [36] J. Alter, F. Lou, A. Rabinowitz, H. Yin, J. Rosenfeld, S.D. Wilton, T.A. Partridge, Q.L. Lu, Systemic delivery of morpholino oligonucleotide restores dystrophin expression bodywide and improves dystrophic pathology, *Nat. Med.* 12 (2006) 175–177.
- [37] T. Yokota, Q.L. Lu, T. Partridge, M. Kobayashi, A. Nakamura, S. Takeda, E. Hoffman, Efficacy of systemic morpholino exon-skipping in Duchenne dystrophy dogs, *Ann. Neurol.* 65 (2009) 667–676.
- [38] M. Ishikawa-Sakurai, M. Yoshida, M. Imamura, K.E. Davies, E. Ozawa, ZZ domain is essentially required for the physiological binding of dystrophin and utrophin to beta-dystroglycan, *Hum. Mol. Genet.* 13 (2004) 693–702.
- [39] A. Aartsma-Rus, I. Fokkema, J. Verschuuren, I. Ginjaar, J. van Deutekom, G.J. van Ommen, J.T. den Dunnen, Theoretic applicability of antisense-mediated exon skipping for Duchenne muscular dystrophy mutations, *Hum. Mutat.* 30 (2009) 293–299.
- [40] A. Aartsma-Rus, C.L. De Winter, A.A. Janson, W.E. Kaman, G.J. Van Ommen, J.T. Den Dunnen, J.C. Van Deutekom, Functional analysis of 114 exon-internal AONs for targeted DMD exon skipping: indication for steric hindrance of SR protein binding sites, *Oligonucleotides* 15 (2005) 284–297.
- [41] L.J. Popplewell, C. Trollet, G. Dickson, I.R. Graham, Design of phosphorodiamidate morpholino oligomers (PMOs) for the induction of exon skipping of the human DMD gene, *Mol. Ther.* 17 (2009) 554–561.
- [42] M. Kinali, V. Arechavala-Gomez, L. Feng, S. Cirak, D. Hunt, C. Adkin, M. Guglieri, E. Ashton, S. Abbs, P. Nihoyannopoulos, M.E. Garralda, M. Rutherford, C. McCulley, L. Popplewell, I.R. Graham, G. Dickson, M.J. Wood, D.J. Wells, S.D. Wilton, R. Kole, V. Straub, K. Bushby, C. Sewry, J.E. Morgan, F. Muntoni, Local restoration of dystrophin expression with the morpholino oligomer AVI-4658 in Duchenne muscular dystrophy: a single-blind, placebo-controlled, dose-escalation, proof-of-concept study, *Lancet Neurol.* 8 (2009) 918–928.
- [43] J.C. van Deutekom, A.A. Janson, I.B. Ginjaar, W.S. Frankhuizen, A. Aartsma-Rus, M. Bremmer-Bout, J.T. den Dunnen, K. Koop, A.J. van der Kooij, N.M. Goemans, S.J. de Kimpe, P.F. Ekhardt, E.H. Venneker, G.J. Platenburg, J.J. Verschuuren, G.J. van Ommen, Local dystrophin restoration with antisense oligonucleotide PRO051, *N Engl J. Med.* 357 (2007) 2677–2686.
- [44] N. Jearawiriyapaisarn, H.M. Moulton, B. Buckley, J. Roberts, P. Sazani, S. Fuchareon, P.L. Iversen, R. Kole, Sustained dystrophin expression induced by peptide-conjugated morpholino oligomers in the muscles of mdx mice, *Mol. Ther.* 16 (2008) 1624–1629.
- [45] P.A. Morcos, Y. Li, S. Jiang, Vivo-Morpholinos: a non-peptide transporter delivers Morpholinos into a wide array of mouse tissues, *Biotechniques* 45 (2008) 613–614 616, 618 passim.
- [46] A. Aartsma-Rus, A.A. Janson, W.E. Kaman, M. Bremmer-Bout, G.J. van Ommen, J.T. den Dunnen, J.C. van Deutekom, Antisense-induced multiexon skipping for Duchenne muscular dystrophy makes more sense, *Am. J. Hum. Genet.* 74 (2004) 83–92.
- [47] L. van Vliet, C.L. de Winter, J.C. van Deutekom, G.J. van Ommen, A. Aartsma-Rus, Assessment of the feasibility of exon 45–55 multiexon skipping for Duchenne muscular dystrophy, *BMC Med. Genet.* 9 (2008) 105.
- [48] A. Exntance, Targeting RNA: an emerging hope for treating muscular dystrophy, *Nat. Rev. Drug Discov.* 8 (2009) 917–918.

In-frame Dystrophin Following Exon 51-Skipping Improves Muscle Pathology and Function in the Exon 52-Deficient *mdx* Mouse

Yoshitsugu Aoki^{1,2}, Akinori Nakamura¹, Toshifumi Yokota^{1,3}, Takashi Saito^{1,4}, Hitoshi Okazawa⁵, Tetsuya Nagata¹ and Shin'ichi Takeda¹

¹Department of Molecular Therapy, National Institute of Neuroscience, National Center of Neurology and Psychiatry (NCNP), Tokyo, Japan;

²Department of System Neuroscience, Medical Research Institute, Tokyo Medical and Dental School University Graduate School, Tokyo, Japan;

³Research Center for Genetic Medicine, Children's National Medical Center, Washington, DC, USA; ⁴Department of Pediatrics, Tokyo Women's Medical University, Tokyo, Japan; ⁵Department of Neuropathology, Medical Research Institute, Tokyo Medical and Dental University, Tokyo, Japan

A promising therapeutic approach for Duchenne muscular dystrophy (DMD) is exon skipping using antisense oligonucleotides (AOs). In-frame deletions of the hinge 3 region of the dystrophin protein, which is encoded by exons 50 and 51, are predicted to cause a variety of phenotypes. Here, we performed functional analyses of muscle in the exon 52-deleted *mdx* (*mdx52*) mouse, to predict the function of in-frame dystrophin following exon 51-skipping, which leads to a protein lacking most of hinge 3. A series of AOs based on phosphorodiamidate morpholino oligomers was screened by intramuscular injection into *mdx52* mice. The highest splicing efficiency was generated by a two-oligonucleotide cocktail targeting both the 5' and 3' splice sites of exon 51. After a dose-escalation study, we systemically delivered this cocktail into *mdx52* mice seven times at weekly intervals. This induced 20–30% of wild-type (WT) dystrophin expression levels in all muscles, and was accompanied by amelioration of the dystrophic pathology and improvement of skeletal muscle function. Because the structure of the restored in-frame dystrophin resembles human dystrophin following exon 51-skipping, our results are encouraging for the ongoing clinical trials for DMD. Moreover, the therapeutic dose required can provide a suggestion of the theoretical equivalent dose for humans.

Received 28 June 2010; accepted 30 July 2010; published online 7 September 2010. doi:10.1038/mt.2010.186

INTRODUCTION

Duchenne muscular dystrophy (DMD) is a severe muscle disorder characterized by mutations in the *DMD* gene that mainly disrupt the reading frame leading to the absence of functional protein.¹ A related allelic disorder, Becker muscular dystrophy (BMD), which shows a much milder phenotype, typically results from shortened but in-frame transcripts of the *DMD* gene that allow expression of limited amounts of an internally truncated but partially functional

protein.² Antisense oligonucleotide (AO)-mediated exon-skipping therapy for DMD, which is a splice modification of out-of-frame dystrophin transcripts, has been demonstrated to exclude specific exons, thereby correcting the translational reading frame, resulting in the production of "Becker-like," shortened but partially functional protein.^{3–7} As a result of exon skipping, DMD could be converted to the milder BMD.⁴

The principle underlying exon-skipping therapy for DMD has been demonstrated in cultured mouse or human cells *in vitro*.^{7–13} In addition, *in vivo* studies in murine or canine animal models have provided preclinical evidence for the therapeutic potential of AO-mediated exon-skipping strategies for DMD.^{14–19} However, the number of patients who have the same mutation as the mice or dogs is estimated to be quite low.^{20,21} On the other hand, a hot spot for deletion mutations between exons 45 and 55 accounts for >60% of DMD patients with deletion mutations.^{20,22} In particular, exon skipping that targets exon 51 is theoretically applicable to the highest percentage (13%) of DMD patients with an out-of-frame deletion mutation.^{20,23–25} Recently, efficient in-frame dystrophin expression following an exon 51-skipping approach has been successfully demonstrated in human subjects using local intramuscular AO injection.^{23,24}

The functionality of the dystrophin protein produced by exon 51-skipping has been inferred by the identification of patients harboring the corresponding in-frame deletions (e.g., in BMD patients).^{6,25} In-frame deletions near hinge 3 (refs. 12,26,27), which is encoded by exons 50 and 51, are predicted to lead to BMD; however, the severity of this disease can vary considerably.^{25,28–32} Consequently, it is desirable to use an animal model to investigate the molecular functionality of in-frame dystrophin lacking hinge 3 following exon 51-skipping. In the exon 52-deficient *mdx* mouse (*mdx52*), exon 52 of the *Dmd* gene has been deleted by gene-targeting, resulting in the production of a premature termination codon in exon 53 (ref. 7,33). This mouse lacks dystrophin and shows dystrophic features as well as muscle hypertrophy.³³ It would be meaningful in predicting whether exon 51-skipping led to an accumulation of BMD-like dystrophin that was able to

Correspondence: Shin'ichi Takeda, Department of Molecular Therapy, National Institute of Neuroscience, National Center of Neurology and Psychiatry (NCNP), 4-1-1 Ogawa-higashi, Tokyo, Japan. E-mail: takeda@ncnp.go.jp

correct the dystrophic histology and muscle function in the *mdx52* mouse.^{11,13,27,34}

Here, we showed the efficient restoration of dystrophin function: the reading frame was restored by exon 51-skipping, and we observed considerable amelioration of the skeletal muscle pathology and function in *mdx52* mice. We describe the first successful effort at systemic rescue of in-frame dystrophin lacking hinge 3 and recovery of muscle function by AO-mediated exon 51-skipping in a mouse model.

RESULTS

Two AOs targeting the 5' and 3' splice sites achieved efficient exon 51-skipping in *mdx52* mice

Skipping exon 51 of the murine *Dmd* gene in the *mdx52* mouse corrects the open-reading frame, resulting in the production of truncated dystrophin that lacks two-thirds of the hinge 3 region and resembles human dystrophin following exon 51-skipping (Figure 1a).^{11,27,34} We first identified effective AO sequences by intramuscular injection into the tibialis anterior (TA) muscles of *mdx52* mice.¹⁴ To optimize the screening dose in the TA muscle, Murine B30 (mB30) AO was injected into 8-week-old *mdx52* mice at doses of 1–10 µg.¹⁵ The mB30 AO designed to skip murine exon 51 was based on human B30 (ref. 11), which targets human exon 51 (Figure 2a). Mice were euthanized 2 weeks after the injection; the TA muscles were isolated and analyzed by reverse transcription (RT)-PCR and immunohistochemistry. Using RT-PCR with primers flanking exons 50 and 53, the cDNA band equivalent to the mRNA missing exons 51 and 52 was detected. We found that

mB30 restored dystrophin expression in a highly dose-dependent manner (Supplementary Figure S1). Then, we designed 13 AO sequences targeting either exonic sequences or exon/intron junctions of murine dystrophin exon 51 (refs. 9,11,35,36). The sequences and compositions of these AOs are described in Table 1 and Figure 2a. We then directly injected one or two of the 14 AOs into the TA muscle of *mdx52* mice. Two weeks after the injection, we analyzed RNA fractions by RT-PCR and cryosections by immunohistochemistry and western blotting. Among the AOs examined, 51D, mB30, and 51I were shown by RT-PCR to be capable of inducing exon 51-skipping at a level approaching 50% (Figure 2b,c). 51D and 51I were designed to target the 5' splice site and an exonic site of exon 51, respectively. It has been reported that a combination of two AOs directed at appropriate motifs in target exons induces more efficient exon skipping than that induced by a single injection.^{34,37} We therefore injected combinations of two AOs into the TA muscles of *mdx52* mice, and found that a combination of two AOs, 51A plus 51D, showed ~75% skipping efficiency, the highest among the combinations that we examined by RT-PCR (Figure 2d,e). 51A is targeted to the 3' splice site of exon 51. We then showed by immunohistochemistry that the combination of 51A plus 51D rendered 50–70% of the fibers dystrophin-positive in cross-sections (Figure 2f), and produced ~50% dystrophin expression on western blots compared with the normal control (Figure 2g). Taking these results together, we concluded that the co-injection of two AOs, 51A plus 51D, was the optimal combination to skip exon 51 of the murine *Dmd* gene.

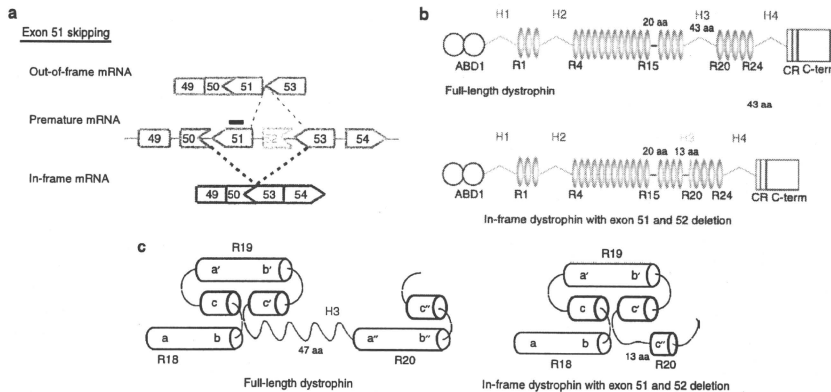


Figure 1 Strategy for exon 51-skipping in *mdx52* mouse. (a) Exon 51-skipping by appropriate phosphorodiamidate morpholino oligomers, indicated by a black line, can restore the reading frame of dystrophin in the *mdx52* mouse, which lacks exon 52 in the mRNA of the murine *Dmd* gene, leading to out-of-frame products. (b) The molecular structure of in-frame dystrophin lacking hinge 3 induced by exon 51-skipping is shown below the full-length dystrophin. The protein contains the actin-binding domain 1 (ABD1) at the N-terminus, the central rod domain containing 24 spectrin-like repeats (R1–24), four hinge domains (H1–4), a 20-amino acid insertion between spectrin-like repeats 15 and 16 (segment 5), the cysteine-rich domain (CR), and the C-terminal domain (C-term). The hinge 3 is encoded by exons 50 and 51; therefore, most of this region is lost after exon 51-skipping in the *mdx52* mouse. (c) Predicted nested repeat model with one long helix, one short helix, and overlap between the “a” helix of the following repeat with the “b” and “c” helices of the preceding repeat, forming the triple helix. The predicted structure of full-length dystrophin (upper) and in-frame dystrophin with exon 51 and 52 deletion (lower).

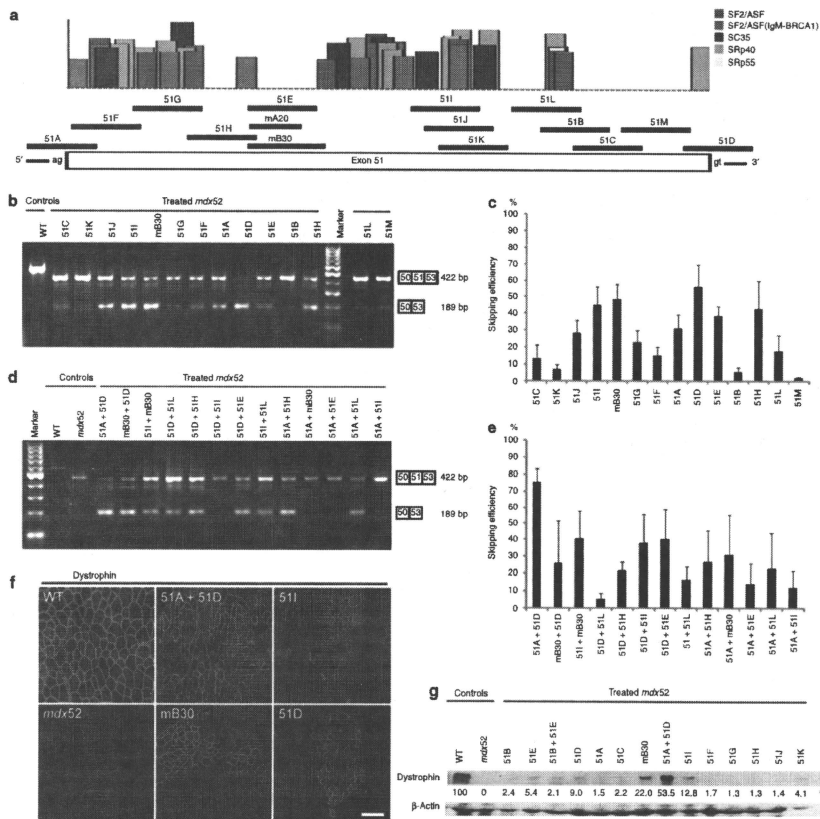


Figure 2 Local intramuscular injection into *mdx52* mice. The restoration of dystrophin in the tibialis anterior (TA) muscles was examined 2 weeks after the injection of 10 μ g of one or a combination of two antisense oligonucleotides (AOs). (a) Fourteen different AOs designed to skip exon 51 of the murine *Dmd* gene. Each AO targets either an exonic splicing enhancer (ESE) or the 5' or 3' splice site, indicated by black lines. The certainties of ESE sites according to ESEfinder 3.0 are indicated by colored boxes. Candidates for splicing enhancer-binding proteins are shown (red, SF2/ASF; purple, SF2/ASF (IgM-BCR1); blue, SC35; green, SRp40; yellow, SRp55). A murine B30 AO (mB30) corresponding to human B30 was designed.¹¹ (b) Effectiveness of the 14 different AOs for exon 51-skipping detected by RT-PCR. Representative data are shown. Skipped products (50–53) are compared with unskipped products (50–51–53). WT, wild-type mouse. (c) Quantitative analysis by RT-PCR of exon 51-skipping by 14 different AOs. The percentages of in-frame transcripts in each lane of b are shown. The data ($n = 3$) are presented as mean \pm SEM. (d) Effectiveness of 13 different combinations of two AOs targeting exon 51 of the murine *Dmd* gene. Representative data are shown. Skipped products (50–53) are compared with unskipped products (50–51–53). *mdx52*, untreated *mdx52* mouse. (e) Quantitative analysis of exon 51-skipping by 13 different combinations of two AOs. The percentages of in-frame transcripts in each lane of d are shown. The data ($n = 3$) are presented as mean \pm SEM. (f) Immunohistochemical staining of dystrophin in TA muscle of WT, untreated and treated *mdx52* mice. The results for AOs 51A plus 51D, 51I, mB30 and 51D are indicated. Dystrophin was detected with a rabbit polyclonal antibody P7. Bar = 100 μ m. (g) Western blotting to detect expression of dystrophin in WT, untreated and treated *mdx52* mice. Representative results for 10 single AOs and three combinations of two AOs. A quantitative analysis (see Materials and Methods) normalized to the expression of β -actin (upper panel), and western blotting to detect β -actin expression (lower panel) are shown. Dystrophin was detected with the Dys2 monoclonal antibody. Note that additional bands between the unskipped and skipped products are visible in some analyses. This is due to heteroduplex formation and has been described previously.¹¹ bp, base pair.

Table 1 Length, annealing coordinates, sequences of all AOs targeting mouse exon 51

AO	Length (bp)	Annealing coordinates	Sequences
51A	25	-18+7	CTGGCAGCTAGTGTTTTGGAAAGAA
51B	25	+171+195	TCACCACCACTCACTCTGTGATT
51C	25	+184+208	ATGTCTTCCAGATCACCCACCATCA
51D	25	+10-15	TGTTTTATCCATACCTCTCTGTTG
51E	25	+66+90	ACAGCAAAGAAGATGGCATTCTAG
51F	25	+3+27	TCACTAGATTAACAGTCTGACTGGC
51G	25	+24+48	CCTTAGTAACACAGATTGTGTCC
51H	25	+47+71	TTCTAGTTGGAGATGACAGTTCC
51I	25	+125+149	CAGCCAGTCTGTAAGTTCTGTCCAA
51J	25	+130+154	AGAGACAGCCAGTCTGAAAGTTCTG
51K	25	+135+159	CAAGCAGAGACAGCCAGTCTGTAAG
51L	25	+162+186	TCACTCTCTGTGATTTATAACTCG
mA20	20	+68+87	GCAAAGAAGATGGCATTCT
mB30	30	+66+95	CTCCAACAGCAAAGAAGATGGCATTCTAG

AOs restored body-wide dystrophin expression in a highly dose-dependent manner in *mdx52* mice

To examine the effect of systemic delivery, we intravenously injected a single dose of 51A plus 51D into 8-week-old *mdx52* mice, at 80 (ref. 15), 160 or 320 mg/kg. Mice were euthanized 2 weeks after the injection; the muscles were isolated and analyzed by RT-PCR and the cryosections by immunohistochemistry. We found that the AOs restored body-wide dystrophin expression in a highly dose-dependent manner, with the 320 mg/kg dose showing ~45% skipping efficiency by RT-PCR (Figure 3a,b) and 45% dystrophin-positive fibers by immunohistochemistry (Figure 3c) in the gastrocnemius (GC) muscle.

Repeated systemic delivery of AOs induced highly efficient in-frame dystrophin in skeletal muscles body-wide

Next, we intravenously injected 320 mg/kg/dose of 51A plus 51D into 8-week-old *mdx52* mice, seven times at weekly intervals. Two weeks after the final injection, whole-body skeletal muscles and the heart were examined. By RT-PCR, we identified cDNA bands corresponding to exon 51 having been skipped in nearly all skeletal muscles of treated mice (Figure 4a). The levels of skipping efficiency were variable: ~67% in the quadriceps (QC), 64% in the GC, 63% in the abdominal, 54% in the paraspinal, 43% in the triceps, 29% in the TA, 24% in the deltoid, 21% in the intercostal, 18% in the diaphragm, and 3% in the heart muscles (Figure 4b). Dystrophin expression was also evaluated by quantitative western blotting (Figure 4c). The expression levels in the QC, GC, and triceps muscles were the highest at 30-40% of normal levels. Those in the TA, intercostal, paraspinal, and diaphragm muscles showed modest expression at 10-20% of normal levels, whereas the dystrophin expression level in the heart was only 1% of normal levels (Figure 4d). We detected 60-80% dystrophin-positive fibers in all skeletal muscles by immunohistochemistry, most prominently in the QC, GC, and paraspinal muscles (Figure 4e). Furthermore,

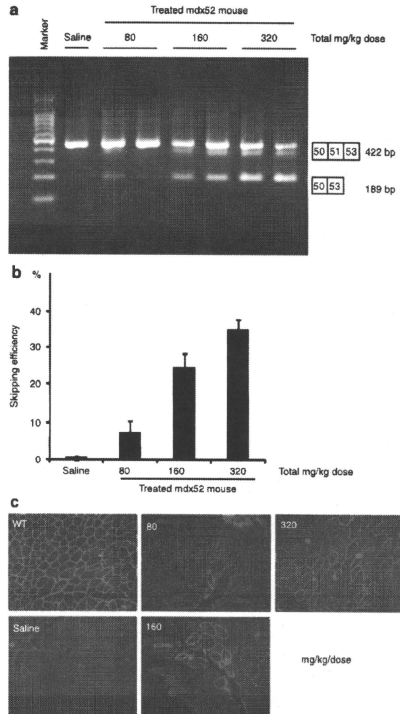


Figure 3 Dose-escalation study of systemic delivery of antisense oligonucleotides (AOs) to *mdx52* mice. Restoration of dystrophin in the gastrocnemius muscle 2 weeks after single intravenous co-injections of 80, 160, or 320 mg/kg/dose of AO. Intravenous saline injection into *Mdx52* mice was used as a control. (a) Detection of exon 51-skipped dystrophin mRNA by RT-PCR. Representative data are shown. Skipped products (50-53) are compared with unskipped products (50-51-53). The additional bands between the unskipped and skipped products is due to heteroduplex formation. (b) Quantitative analysis of exon 51-skipping by AO. The percentages of in-frame transcripts are shown. The data (n = 3) are presented as mean ± SEM. (c) Immunohistochemical staining of dystrophin in the quadriceps muscles of a treated *mdx52* mouse. Dystrophin was detected with rabbit polyclonal antibody P7. Bar = 100 μm. bp, base pair.

most of the nonpositive fibers in our study showed weak dystrophin signals.

We examined the expression of components included in the *dystrophin*-glycoprotein complex in the QC by immunohistochemistry. The expression of α-sarcoglycan correlated well with that of dystrophin (Figure 4f). We also observed the recovery of β-dystroglycan and α1-syntrophin expression at

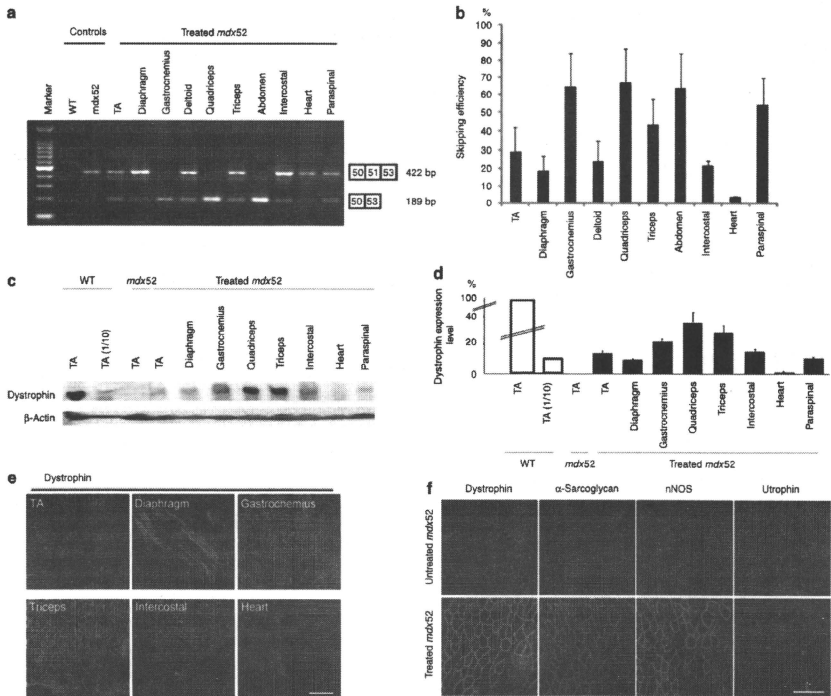


Figure 4 Repeated systemic delivery of antisense oligonucleotides (AOs) to *mdx52* mice. The restoration of dystrophin in various muscles after seven weekly intravenous co-injections of 320 mg/kg/dose of AOs was examined. (a) Detection of exon 51-skipped dystrophin mRNA by RT-PCR. Representative data are shown. Skipped products (50-53) are compared with unskipped products (50-51-53). The additional bands between unskipped and skipped products is due to heteroduplex formation. (b) Quantitative analysis of exon 51-skipping by AOs. The percentages of in-frame transcripts are shown. The data ($n = 3$) are presented as mean \pm SEM. (c) Western blotting after AO injections to detect the expression of dystrophin (upper panel) and β -actin (lower panel) in the TA, diaphragm, gastrocnemius, quadriceps, triceps brachii, intercostal, heart, and paraspinal muscles of a treated *mdx52* mouse. Representative results are shown. Dystrophin was detected with the Dys2 monoclonal antibody. (d) Quantitative analysis of dystrophin expression after AO injection. The data ($n = 4$) are presented as mean \pm SEM. TA(1/10): 10% of WT samples. (e) Immunohistochemical staining of dystrophin in the TA, diaphragm, gastrocnemius, triceps brachii, intercostal, and heart muscles of a treated *mdx52* mouse. Dystrophin was detected with rabbit polyclonal antibody P7. Bar = 100 μ m. (f) Immunohistochemical staining of dystrophin, α -sarcoglycan, neuronal nitric oxide synthase (nNOS) and utrophin in the quadriceps muscle of an untreated *mdx52* mouse (upper panel) and a treated *mdx52* mouse (lower panel). Bar = 100 μ m. *mdx52*, untreated *mdx52* mouse; TA, tibialis anterior; WT, wild-type mouse.

the sarcolemma (data not shown). On the other hand, utrophin expression was diminished in dystrophin-positive fibers (Figure 4f).

In-frame dystrophin largely lacking hinge 3 ameliorated skeletal muscle pathology

The *mdx52* mice skeletal muscle shows hypertrophy and an increased ratio of centrally nucleated fibers.¹⁷ Two weeks after seven consecutive weekly i.v. injections of the combination of AOs, the wet weight of the extensor digitorum longus muscle

tended to be slightly lower in treated mice than in untreated mice (Figure 5a). We observed less muscle degeneration and fewer cellular infiltrates in the treated TA muscle compared with the untreated TA muscle (Figure 5b). We then evaluated the detailed histological changes in the treated muscles and compared them with the changes in the untreated muscles. The fiber size variation in the treated TA muscle was less than that in the untreated TA muscle (Figure 5c). We found a significant decrease in the mean cross-sectional area of muscle fibers in treated mice compared with those in untreated mice (Figure 5d). The percentages

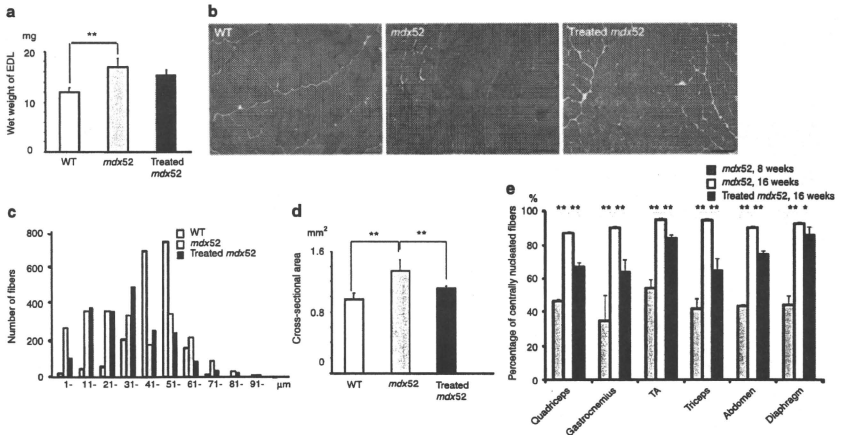


Figure 5 Amelioration of pathology in body-wide muscles of *mdx52* mice after seven weekly intravenous co-injections of 320 mg/kg/dose of antisense oligonucleotides. (a) Wet weight of the extensor digitorum longus (EDL) muscles of wild-type (WT), untreated and treated 16-week-old *mdx52* mice. The data ($n = 4$) are presented as mean \pm SEM. $**P < 0.01$. (b) Hematoxylin and eosin staining of cryosections in tibialis anterior (TA) muscle of WT, untreated and treated *mdx52* mice. Bar = 100 μ m. (c) Histogram of muscle fibers in the TA muscle of WT, untreated and treated 16-week-old *mdx52* mice. (d) Cross-sectional area of EDL muscles of WT, untreated and treated 16-week-old *mdx52* mice. The data ($n = 4$) are presented as mean \pm SEM. $**P < 0.01$. (e) The ratio of centrally nucleated fibers in the quadriceps, gastrocnemius, TA, triceps brachii, abdominal, and diaphragm muscles of untreated 8-week-old (dark gray), 16-week-old *mdx52* mice (light gray), and treated 16-week-old *mdx52* mice (black). The data ($n = 4$) are presented as mean \pm SEM. $*P < 0.05$; $**P < 0.01$. *mdx52*, untreated *mdx52* mouse.

of centrally nucleated fibers were lower in the triceps, GC, QC, and abdominal muscles than in the diaphragm and TA muscles (Figure 5e). These changes reflect the amelioration of muscle fiber hypertrophy and dystrophic changes in the treated *mdx52* mice.

In-frame dystrophin largely lacking hinge 3 restored skeletal muscle function

To examine the function of the AO-induced dystrophin, we evaluated skeletal muscle function with a battery of tests after seven weekly i.v. AO injections. The protection of muscle fibers against degeneration was supported by a significant reduction in serum creatine kinase levels in the treated mice (Figure 6a). Significant improvements in treadmill endurance (Figure 6b), maximum forelimb grip force (Figure 6c), and specific tetanic force of the extensor digitorum longus muscle (Figure 6d) were observed in treated *mdx52* mice compared with nontreated *mdx52* mice.

Efficacy of repeated AO injection in *mdx52* mice confirmed by gene expression array

Gene expression array analysis has been widely used to profile gene expression for disease diagnosis and therapy due to its ability to interrogate every transcript in the genome simultaneously. Dystrophic TA muscle has been compared with normal TA muscle in human and *mdx* mice at various stages of the

disease.^{23,24} To evaluate the gene expression profile of TA muscles following exon 51-skipping, we performed genome-wide gene expression analysis (Figure 7a). Gene expression array analysis showed that the gene expression profiles of TA muscles correlated well between the treated and untreated *mdx52* mice ($r^2 = 0.97$), and there was no unexpected downregulation of housekeeping genes or upregulation of stress-related proteins. We found that dystrophin-associated proteins such as dystrophin, neuronal nitric oxide synthase, and $\alpha 1$ -syntrophin were upregulated, α -sarcoglycan and β -dystroglycan levels were unchanged, and utrophin was downregulated. We also found that inflammatory cytokines were downregulated in treated *mdx52* mice. Quantitative RT-PCR following gene expression array analysis showed that dystrophin and neuronal nitric oxide synthase expression levels were 3.4 and 1.9 times higher than those in the untreated *mdx52* mice, respectively; however, they were still only 33 and 40% of the normal levels, respectively (Figure 7b). Utrophin expression levels were upregulated in the untreated *mdx52* mice, but downregulated in the treated *mdx52* mice compared with wild-type (WT) mice (Figure 7b). In treated *mdx52* mice, we observed reduced levels of several C-C class chemokine ligands (Ccl) such as Ccl7, Ccl21b, and Ccl2, which are small cytokines that induce the migration of monocytes and other cell types such as natural killer cells and dendritic cells (Figure 7c). This might reflect an improvement of the muscle inflammatory response in the treated *mdx52* mice.

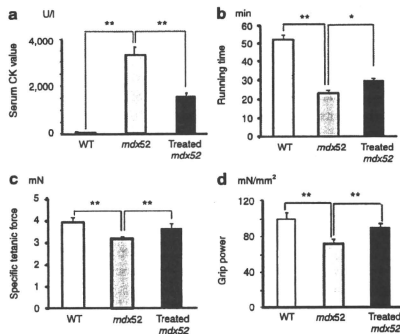


Figure 6 Muscle function in *mdx52* mice after seven weekly intravenous co-injections of 320 mg/kg/dose of antisense oligonucleotides. (a) Measurement of serum creatine kinase (CK) levels (IU/l). (b) Treadmill performance (min), (c) grip power test (mN/g), and (d) specific tetanic force of the extensor digitorum longus muscle (mN/mm²). Wild-type (WT), untreated (*mdx52*), and treated 16-week-old *mdx52* mice were examined. The data ($n = 4$) are presented as mean \pm SEM. * $P < 0.05$; ** $P < 0.01$.

No detectable toxicity after repeated delivery of AOs into *mdx52* mice

No signs of illness and no deaths were noted during the period of AO treatment. To further monitor any potential toxicities in the major organs induced by treatment with AOs, we compared a series of serum markers commonly used as indicators of liver and kidney dysfunction in WT, untreated and treated *mdx52* mice. No significant differences were detected among the three groups in the levels of creatinine, blood urea nitrogen, aspartate amino transferase, alanine aminotransferase, total bilirubin, alkaline phosphatase, and γ -glutamyl transpeptidase (Supplementary Figure S2a). Histological examination of liver and kidney revealed no signs of tissue damage or increased monocyte infiltrations in treated *mdx52* mice (Supplementary Figure S2b). These data confirm that this AO combination was nontoxic in this study.

In vitro exon 51-skipping in DMD 5017 cells with deletion of exons 45–50

We newly designed several AOs based on murine sequences: hAc (51Ac) targeting the 5' splice site, and hDo1 (51D1) and hDo2 (51D2) targeting the 3' splice site of human exon 51. The sequences and composition of the AO treatments are described in Supplementary Table S1. MyoD-converted fibroblasts (DMD 5017 cells) were examined after 48-hour incubation with a single or two AOs at a final concentration of 1, 5, or 10 μ M. Among the AOs examined, hAc plus hDo1, and B30 alone, were shown by RT-PCR to be capable of inducing exon 51-skipping at a level approaching 50 and 30%, respectively (Supplementary Figure S3). On the other hand, hAc, hDo1, or hDo2 alone were less effective at inducing exon 51-skipping (Supplementary Figure S3). These

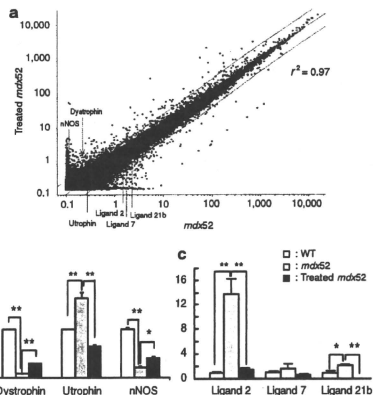


Figure 7 Genome-wide expression analyses by gene expression array using tibialis anterior muscles. Gene expression array analysis after repeated intravenous co-injections of 320 mg/kg/dose of antisense oligonucleotides into *mdx52* mice. (a) A scatter plot of global gene expression analyses by gene expression array in treated and untreated *mdx52* mice. The upper line shows twofold changes and the lower line shows 0.5-fold changes in gene expression levels between treated and untreated *mdx52* mice. The positions of dystrophin, utrophin, neuronal nitric oxide synthase (nNOS), and the C-C class chemokine ligands (CCLs) 2, 7, and 21b are indicated. (b,c) The gene expression levels of dystrophin, utrophin, nNOS (b) and CCLs 2, 7, and 21b (c) by quantitative PCR, in 16-week-old WT, untreated and treated *mdx52* mice. The data ($n = 3$) are presented as mean \pm SEM. * $P < 0.05$; ** $P < 0.01$. *mdx52*, untreated *mdx52* mouse; WT, wild-type mouse.

results suggest that the co-injection of two AOs could induce highly effective exon 51-skipping in DMD cells.

DISCUSSION

This is the first report showing widespread induction of in-frame dystrophin lacking most of hinge 3 following exon 51-skipping, and clear recovery of muscle function to therapeutic levels in a DMD mouse model.

Exon skipping produces several forms of in-frame dystrophin that lack part of the molecular structure depending on the targeted exons.⁴⁻⁶ The molecular structure of dystrophin is composed of the actin-binding domain 1 at the N-terminus (ABD1), the central rod domain containing 24 spectrin-like repeats (R1–24), four hinge domains, a 20-amino acid insertion between spectrin-like repeats 15 and 16 (segment 5), the cysteine-rich domain, and the C-terminal domain (Figure 1b).^{27,38} Until now, the in-frame dystrophin formed following exon 23-skipping, which lacks half of the 6th spectrin-like repeat and part of the 7th, ameliorated the muscle pathology and function in *mdx* mice with a point mutation in exon 23 (refs. 15,16). These results were consistent with the fact that in-frame deletions of the central rod domain in humans typically lead to a mild BMD.⁴ However, the severity of BMD with in-frame deletions including hinge 3 can vary considerably.^{28-32,38}

The hinges are proline-rich, nonrepeat segments that may confer flexibility to dystrophin.²⁷ Among them, the hinge 3 region is encoded by exons 50 and 51, located between the 19th and 20th spectrin-like repeats, and is prone to deletion mutations.^{20,22} Recently, it was reported that hinge 3 is more important than hinge 2 in preventing muscle degeneration and promoting muscle maturation in the microdystrophin^{Δ84-823}/*mdx* transgenic mice.³⁸ The in-frame dystrophin produced following exon 51-skipping is predicted to lack most of the hinge 3 region (Figure 1b); hinges 1, 2, 3, and 4 consist of 75, 50, 43, and 72 amino acid residues, respectively.^{27,28} The small segment of hinge 3 that remains following exon 51-skipping consists of 13 amino acid residues with two prolines and would not be predicted to function as a hinge (Figure 1c). This remaining fragment is very similar to segment 5, which consists of 20-amino acid residues with one proline and is located between the 15th and 16th spectrin-like repeats.²⁷ Based on the molecular structure of dystrophin, the small segment of the hinge 3 might act as a "turn," which is bound to the helix of the 20th repeat.^{27,28} Our results suggest that the hinge 3 region is more essential in the short microdystrophin (167 kDa) than in the almost full-length dystrophin lacking hinge 3 due to exon 51-skipping (420 kDa).^{38,39}

In-frame dystrophin expression in skeletal muscle at 20% of normal levels produced moderate/mild BMD phenotypes.²⁶ Moreover, restoration of 20–30% in-frame dystrophin expression resulted in protection from muscle degeneration and recovery of skeletal muscle function in the transgenic *mdx* mouse.⁴⁰ As a first step, we screened optimal AO sequences including mB30 for skipping of exon 51 to induce in-frame dystrophin at up to 20% of normal dystrophin levels. To date, specific AO sequences have been assessed for their efficiency of exon skipping using cell-based experimental systems, with the optimal sequences then used for *in vivo* experiments.^{11,41,42} However, the *in vivo* efficacy of phosphorodiamidate morpholino oligomers (PMOs), which are rather difficult to deliver into mammalian cells in culture because of their neutral chemistry,^{11,19} could differ from that *in vitro*.¹⁴ Therefore, we used the *mdx52* mouse to screen AO sequences for exon 51-skipping by intramuscular injection *in vivo*. We also showed that simultaneous delivery of two AO sequences directed against both the 3' and the 5' splice sites drove skipping of exon 51 more efficiently than any single or two AO sequences targeting exonic regions in the *mdx52* mouse. This combination of AOs worked in a synergistic fashion, where the increase in activity was greater than the additive effect of each individual AO.^{14,24,37}

We found that the skipping efficiency induced by systemically delivered PMO increased in proportion to the AO dose in the *mdx52* mouse. A dose-dependent restoration of dystrophin expression in the muscles of *mdx* mice by systemically delivered PMO has also been reported.⁴³ The therapeutic dose (320 mg/kg/dose) of exon 51-skipping AOs in the *mdx52* mouse to induce 20–30% of normal dystrophin levels is approximately four times as much as the dose (80 mg/kg/dose) required for exon 23-skipping in the *mdx* mouse. We have to consider the possibility that the difference of the genetic background of mice between *mdx52* (C57BL/6j) and *mdx* (C57BL/10) mice could influence the properties of exon skipping. Our results suggest that the therapeutic dose of AO required is different depending on which exon is being targeted. Because

AO-mediated exon skipping is the first RNA-modulating therapeutic with this mechanism of action, this study using a DMD mouse model could provide a suggestion for human equivalent doses based on body surface area.⁴⁴ Recently, press releases from both Prosenza for PRO051 and AVI Biopharma for AVI-4658 have revealed that DMD patients who received 2–6 and 2–20 mg/kg, respectively, induced specific exon 51-skipping and dystrophin expression in a dose-related manner (<http://www.prosenza.eu/press-room/press-releases/2009-09-14-PRO051-shows-favourable-results.php>; <http://investorrelations.avibio.com/phoenix.zhtml?c=64231&p=irol-newsArticle&ID=1433350&highlight=>).

In this study, the dystrophin expression level in treated *mdx52* mice was restored to roughly 20–30% of normal levels, and creatine kinase levels and skeletal muscle function significantly recovered in the treated mice. These findings show that the in-frame dystrophin lacking most of hinge 3 ameliorates dystrophic histology and functional phenotypes in *mdx52* mice as well as the dystrophin produced following exon 23-skipping or microdystrophin in *mdx* mice.^{15,16} On the other hand, the treadmill endurance of the treated *mdx52* mice was still considerably inferior to that of WT mice compared with the clear recovery of forelimb grip force and specific tetanic force of the extensor digitorum longus muscle. These findings are similar to the data produced using microdystrophin in the *mdx* mouse.³⁹ Two possibilities remain to explain the incomplete recovery: insufficient dystrophin expression or defective dystrophin molecular structure due to exon 51-skipping. To examine these possibilities, we are now trying to increase the level of dystrophin expression using a high dose of PMO and using peptide-conjugated PMO in *mdx52* mice.

The amelioration of the histopathology demonstrated by the reduction of centrally nucleated fibers in treated *mdx52* mice was marked in the muscles with high levels of dystrophin expression, and the effect was modest in the muscles with low levels of dystrophin, in accordance with a previous report.^{15,16} It is noteworthy that high levels of dystrophin expression were seen in severely degenerated muscles, and that low levels of expression were found in less affected muscles. We suggest the possibility that the anti-gravity muscles, such as the QC, GC, triceps brachii, abdominal, and paraspinal muscles⁴⁵ efficiently incorporated PMO into the muscle fibers. We showed that the anti-gravity muscles were mainly affected in *mdx52* mice during the period that we examined; therefore, those severely affected muscles had taken up the most AO. Our data support the fragile membrane hypothesis that has been proposed as the background for PMO incorporation into dystrophic muscle.^{46,47} This hypothesis also explains the inefficient incorporation of PMO into the diaphragm muscle where dystrophin changes chronically persisted, as previously reported.^{15,16}

To screen for changes in gene expression levels influenced by the in-frame dystrophin, we performed gene expression array analysis. The inflammatory chemokines Ccl2, Ccl7, and Ccl21b, which were downregulated after treatment, play important roles in the migration of macrophages, CD4⁺ and CD8⁺ T cells to muscle in *mdx* mice.⁴⁸ It is also known that depletion of these cells from *mdx* mice decreased the sarcolemmal damage.⁴⁹ These data showed that the inflammatory process, which could aggravate the pathology, was prevented in *mdx52* mice. Measurement of the chemokines might be a beneficial index of the therapeutic effects on *mdx52* mice.

In conclusion, this report describes the first successful effort at systemic rescue of in-frame dystrophin lacking most of hinge 3 and muscle function by PMO-mediated exon 51-skipping in a mouse model. Because the structure of the in-frame dystrophin lacking most of hinge 3 in mice resembles human dystrophin following exon 51-skipping, our results are extremely encouraging as regards the ongoing systemic clinical trials for DMD. In addition, the therapeutic dose in DMD model mice provides a suggestion of the theoretical equivalent dose in humans.

MATERIALS AND METHODS

Animals. Exon 52-deficient X chromosome-linked muscular dystrophy (*mdx52*) mice were produced by a gene-targeting strategy and maintained at our facility.¹³ The mice have been backcrossed to the C57BL/6J WT strain for more than eight generations. Eight-week-old male *mdx52* and WT mice were used in this study. All experimental protocols in this study were approved by The Experimental Animal Care and Use Committee of the National Institute of Neuroscience, National Center of Neurology and Psychiatry (NCNP), Tokyo, Japan.

Antisense sequences and delivery methods. Thirteen AOs for targeted skipping of exon 51 during dystrophin pre-mRNA splicing in mice were comprehensively designed to anneal to the 5' splice site (51A), the 3' splice site (51D), and other intraxonic regions (51B, 51C, 51E, 51F, 51G, 51H, 51I, 51J, 51K, 51L, 51M). The sequences and positions of the AOs are described in Table 1. mB30, which corresponds to human B30, was also specifically designed for this study.¹¹ To design these sequences, we referred to previously published sequences and considered GC content and secondary structure to avoid self- and heterodimerization.^{11,12} All sequences were synthesized using a morpholino backbone (Gene Tools, Philomath, OR). Primers for RT-PCR and sequencing analysis were synthesized by Operon Biotechnologies (Tokyo, Japan) and are listed in **Supplementary Table S1**.

Ten micrograms of PMO were injected into each TA muscle of *mdx52* mice. Muscles were obtained 2 weeks after the intramuscular injection. To examine the optimal therapeutic dose, a total of 80 (ref. 15), 160 or 320 mg/kg/dose of AO was injected into the tail vein of *mdx52* mice singly. Muscles were isolated 2 weeks after the systemic injection and analyzed by RT-PCR and the cryosections by immunohistochemistry. Following the dose-escalation study, a 320 mg/kg dose of PMO in 200 μ l of saline,¹⁹ or 200 μ l saline, was injected into the tail vein of *mdx52* mice or WT mice, seven times at weekly intervals. The mice were examined 2 weeks after the final injection. Muscles were dissected immediately, snap-frozen in liquid nitrogen-cooled isopentane and stored at -80°C for RT-PCR, immunohistochemistry, western blotting, and gene expression array analysis. Liver and kidney were also frozen in liquid nitrogen and stored at -80°C for pathological analysis.

RT-PCR and sequencing of cDNA. Total RNA was extracted from cells or frozen tissue sections using TRIzol (Invitrogen, Carlsbad, CA) from treated *mdx52* mice, and from WT and untreated *mdx52* mice, which were used as controls, respectively. Two hundred nanograms of total RNA template was used for RT-PCR with a QuantiTect Reverse Transcription kit (Qiagen, Crawley, UK) according to the manufacturer's instructions. The cDNA product (1 μ l) was then used as the template for PCR in a 25 μ l reaction with 0.125 units of TaqDNA polymerase (Qiagen). The reaction mixture comprised 10 \times PCR buffer (Roche, Basel, Switzerland), 10 mmol/l of dNTP (Qiagen), and 10 μ mol/l of each primer. The primer sequences were Ex50F 5'-TTTACTTCGGGAGCTGAGGA-3' and Ex53R 5'-ACCTGTTGGGCTTCTTCTT-3' for amplification of cDNA from exons 50-53. The cycling conditions were 95 $^{\circ}\text{C}$ for 4 minutes, then 35 cycles of 94 $^{\circ}\text{C}$ for 1 minute, 60 $^{\circ}\text{C}$ for 1 minute, 72 $^{\circ}\text{C}$ for 1 minute, and finally 72 $^{\circ}\text{C}$ for 7 minutes. The intensity of PCR bands was analyzed by

using ImageJ software (<http://rsbweb.nih.gov/ij/>), and skipping efficiency was calculated by using the following formula [(the intensity of skipped band) / (the intensity of skipped band + intensity of unskipped band)].²¹ After the resulting PCR bands were extracted using a gel extraction kit (Qiagen), direct sequencing of PCR products was performed by the Biomatrix Laboratory (Chiba, Japan).

Immunohistochemistry, and hematoxylin and eosin staining. At least ten 8 μ m cryosections were cut from flash-frozen muscles at 100 μ m intervals. The serial sections were stained with polyclonal rabbit antibody P7 against the dystrophin rod domain (a gift from Qi-Long Lu, Carolinas Medical Center, Charlotte, NC), anti- α -sarcoglycan monoclonal rabbit antibody (Novocastra Laboratories, Newcastle, UK), anti- β -dystroglycan monoclonal mouse antibody (Novocastra Laboratories), anti- α 1-syntrophin monoclonal mouse antibody (Novocastra Laboratories), antineuronal nitric oxide synthase polyclonal rabbit antibody (Zymed, San Francisco, CA), and anti-trophin polyclonal rabbit antibody (UT-2). Alexa-488 or 568 (Molecular Probes, Cambridge, UK) was used as a secondary antibody. 4',6-diamidino-2-phenylindole containing a mounting agent (Vectashield; Vector Laboratories, Burlingame, CA) was used for nuclear counterstaining. The maximum number of dystrophin-positive fibers in one section was counted, and the TA muscle fiber sizes were evaluated using a BZ-9000 fluorescence microscope (Keyence, Osaka, Japan). Hematoxylin and eosin (H&E) staining was performed using Harris H&E.

Western blotting. Muscle protein from cryosections was extracted with lysis buffer as described previously.¹⁴ Two to twenty micrograms of protein were loaded onto a 5-15% XV Pantera Gel (DRC, Tokyo, Japan). The samples were transferred onto an Immobilon polyvinylidene fluoride membrane (Millipore, Billerica, MA) by semidry blotting at 5 mA/cm² for 1.5 hours. The membrane was incubated with the C-terminal monoclonal antibody Dys2 (Novocastra) at room temperature for 1 hour. The bound primary antibody was detected by horseradish peroxidase-conjugated goat anti-mouse IgG (Cedarlane, Burlington, ON) and SuperSignal chemiluminescent substrate (Pierce, Rockford, IL). Anti- β -actin antibody was used as a loading control. Signal intensity of detected bands of the blots were quantified using ImageJ software and normalized to the loading control.

Serum creatine kinase levels and toxicity tests. Four treated *mdx52* mice were examined for toxic effects of PMO before injection, 1 week after the third injection, and 2 weeks after the last injection. Blood was taken from the tail artery and centrifuged at 3,000g for 10 minutes. The biochemical markers creatine kinase, electrolytes (sodium, potassium, and chloride ions), blood urea nitrogen, total bilirubin, alkaline phosphatase, aspartate transaminase, and alanine transaminase were assayed as described previously.¹⁴ The histology of the liver, lung, and kidney was examined microscopically on cryosections.

Functional testing. The mice were placed on a flat MK-680S treadmill (Muromachi Kikai, Tokyo, Japan) and forced to run at 5 m/minute for 5 minutes. After 5 minutes, the speed was increased by 1 m/minute every minute. The test was stopped when the mouse was exhausted and did not attempt to remount the treadmill, and the time to exhaustion was determined.

The grip strength of the mice was assessed by a grip strength meter (MK-380M; Muromachi Kikai). The mice were held 2 cm from the base of the tail, allowed to grip a woven metal wire with their forelimbs, and pulled gently until they released their grip. Five sequential tests for the exerted force were carried out for each mouse, with 5-second intervals, and the data were averaged.

The extensor digitorum longus muscles were kept in Krebs-Henseleit solution at 25 $^{\circ}\text{C}$ and stimulated with a pair of platinum electrodes using an electronic stimulator (SEN-3301; Nihon Kohden, Tokyo, Japan). A Thermal Arrayorder (WR300; Graphtec, Yokohama, Japan) was used to

control the stimulation and to record the force of the muscle contraction. Measurement of the specific tetanic force was performed as previously described.²⁹

Gene expression array analysis. TA muscles from treated *mdx52*, age-matched WT, and untreated *mdx52* mice ($n = 3$ each) were used for these experiments. Total RNA was purified using an RNeasy mini kit (Qiagen) according to the manufacturer's protocol. Gene expression array analysis was performed by the branch of the Agilent Technologies (Santa Clara, CA) in Japan. Three whole mouse genome oligo microarrays 44K (Agilent Technologies) were used in this study. Global normalization was performed to compare genes from chip to chip using GeneSpring 9.0 (Tomy Digital Biology, Denver, CO). All data quality controls were performed and met the Affymetrix quality assessment guidelines. Data analysis was performed using GeneSpring 9.0 (Tomy Digital Biology). Differentially expressed genes were selected if they passed Welch's *t*-test, a parametric test in which the variance is not assumed to be equal. $P < 0.01$ (with correction for multiple testing by the Benjamini and Hochberg method for the false discovery rate) and a 5% cutoff were used; a change of at least twofold between any two of the groups used in this study was considered significant.

Quantitative real-time PCR. For genes selected for the gene expression array, we used the same RNA that was isolated for the gene expression array and prepared cDNA using SuperScript III Reverse Transcriptase (Invitrogen). Real-time PCR was performed using a SYBR Premix Ex Taq II kit (Takara, Tokyo, Japan). Expression values were normalized to 18S rRNA expression and shown as a fold increase in the treated *mdx52*, untreated *mdx52*, and age-matched WT samples.

Transfection of cultured cells with AO. DMD 5017 cells were obtained from Coriell Cell Repositories (Camden, NJ). Fibroblasts were cultured in 20% growth medium, containing Dulbecco's modified Eagle's medium and F-12 in a 1:1 mixture (Invitrogen), 20% fetal bovine serum (SABC Biosciences, Lenexa, KS) and 1% penicillin/streptomycin (Sigma-Aldrich, St. Louis, MO). Then, fluorescence-activated cell sorting sorted MyoD-enhanced green fluorescent protein-positive fibroblasts (MyoD-converted fibroblasts) were cultured in differentiation medium, containing Dulbecco's modified Eagle's medium/F-12 in a 1:1 mixture (Invitrogen), 2% horse serum (Invitrogen), and 1% penicillin/streptomycin (Sigma-Aldrich). hDo1, hDo2, and hAc were designed (Table 1) and synthesized by Gene Tools. MyoD-converted fibroblasts were transfected with a single or two AOs at a final concentration of 10 $\mu\text{mol/L}$. EndoPorter (Gene Tools) was added to give a final concentration of 6 $\mu\text{mol/L}$. After 48-hour incubation with the AOs, total RNA was extracted from MyoD-converted fibroblasts using Trizol (Invitrogen).

Statistical analysis. Statistical differences were assessed by one-way analysis of variance with differences among the groups assessed by a Tukey comparison. All data are reported as mean values \pm SEM. The level of significance was set at $P < 0.05$.

SUPPLEMENTARY MATERIAL

Figure S1. Dose-escalation study of exon 51-skipping by local intramuscular injection into *mdx52* mice.

Figure S2. Examination of adverse effects after systemic delivery of antisense oligonucleotides (AOs).

Figure S3. *In vitro* exon 51-skipping in DMD 5017 cells with deletion of exons 45–50.

Table S1. Length, annealing coordinates, sequences of all AOs targeting human exon 51.

ACKNOWLEDGMENTS

We thank Eric Hoffman and Terence Partridge for insightful discussions about this study. We thank Kouichi Tanaka and Hiroko Hamazaki for their support, and Mikiharu Yoshida, Michihiro Imamura, Masanori

Kobayashi, Jing Hong Shin, Yuko Shimizu, Norio Motohashi, Erika Yada, Katsutoshi Yuasa, and Morizono Hiroki for useful discussions and technical assistance. We thank Qi-Long Lu for supplying the antibody to dystrophin (P7). This work was supported by Grants-in-Aid for Research on Nervous and Mental Disorders (19A-7), Health and Labor Sciences Research Grants for Translation Research (H19-Translational Research-003 and H21-Clinical Research-015), and Health Sciences Research Grants for Research on Psychiatry and Neurological Disease and Mental Health (H18-kokoro-019) from the Ministry of Health, Labour and Welfare of Japan. This work was performed in Kodaira, Tokyo, Japan.

REFERENCES

- Hoffman EP, Brown RH Jr and Kunkel LM (1987). Dystrophin: the protein product of the Duchenne muscular dystrophy locus. *Cell* 51: 919–928.
- Monaco AP, Bertelson C, Liechi-Gallati S, Moser H and Kunkel LM (1988). An explanation for the phenotypic differences between patients bearing partial deletions of the DMD locus. *Genomics* 2: 90–95.
- Wilton SD, Fall AM, Harding PL, McCloy G, Coleman C and Fletcher S (2007). Antisense oligonucleotide-induced exon skipping across the human dystrophin gene transcript. *Mol Ther* 15: 1288–1296.
- Aartsma-Rus A, Bremner-Bout M, Janson AA, Ginjaar IB, Baas F, den Dunnen JT et al. (2002). Targeted exon skipping as a potential gene correction therapy for Duchenne muscular dystrophy. *Neuromuscul Disord* 12 Suppl 1: S71–S77.
- Matsuura M, Masumura T, Nishio H, Nakajima T, Kitoh Y, Takumi T, et al. (1991). Exon skipping during splicing of dystrophin mRNA precursor due to an intron deletion in the dystrophin gene of Duchenne muscular dystrophy kobe. *J Clin Invest* 87: 2127–2131.
- Muntoni F, Torelli S, and Ferlini A (2003). Dystrophin and mutations: one gene, several proteins, multiple phenotypes. *Lancet Neurol* 2: 731–740.
- Dunndorf MG, Manoharan M, Villegas P, Ezeon JC and Dickson G (1998). Modification of splicing in the dystrophin gene in cultured MDX muscle cells by antisense oligonucleotides. *Hum Mol Genet* 7: 1083–1090.
- van Deutekom JC, Bremner-Bout M, Janson AA, Ginjaar IB, Baas F, den Dunnen JT et al. (2005). Antisense-induced exon skipping restores dystrophin expression in DMD patient derived muscle cells. *Hum Mol Genet* 10: 1547–1554.
- Aartsma-Rus A, De Winter CL, Janson AA, Kaman WE, Van Ommeren GJ, Den Dunnen JT et al. (2005). Functional analysis of 114 exon-internal AONs for targeted DMD exon skipping: indication for steric hindrance of 58 protein binding sites. *Oligonucleotides* 15: 284–297.
- Wilton SD, Lloyd F, Carville K, Fletcher S, Honeyman K, Agrawal S, et al. (1999). Specific removal of the nonsense mutation from the mdx dystrophin mRNA using antisense oligonucleotides. *Neuromuscul Disord* 9: 330–338.
- Archavala-Gomez Y, Graham IR, Popplewell JL, Adams AM, Aartsma-Rus A, Kinali M, et al. (2007). Comparative analysis of antisense oligonucleotide sequences for targeted skipping of exon 51 during dystrophin pre-mRNA splicing in human muscle. *Hum Gene Ther* 18: 798–810.
- Beggs AH, Hoffman EP, Snyder JR, Arakata K, Specht L, Shapiro F, et al. (1991). Exploring the molecular basis for variability among patients with Becker muscular dystrophy: dystrophin gene and protein studies. *Am J Hum Genet* 49: 54–67.
- Aartsma-Rus A, Janson AA, Kaman WE, Bremner-Bout M, den Dunnen JT, Baas F, et al. (2003). Therapeutic antisense-induced exon skipping in cultured muscle cells from six different DMD patients. *Hum Mol Genet* 12: 907–914.
- Yokota T, Lu Q, Partridge T, Kobayashi M, Nakamura A, Takeda S, et al. (2009). Efficacy of systemic morpholino exon-skipping in Duchenne dystrophy dogs. *Ann Neurol* 65: 667–676.
- Alter J, Lou F, Rabinowitz A, Yin H, Rosenfeld J, Wilton SD, et al. (2006). Systemic delivery of morpholino oligonucleotide restores dystrophin expression bodywide and improves dystrophy pathology. *Nat Med* 12: 175–177.
- Lu Q, Mann C, Lou F, Ravi-Chandar G, Morris CG, Xu SA, et al. (2003). Functional actions of dystrophin produced by skipping the mutated exon in the mdx dystrophic mouse. *Nat Med* 9: 1009–1014.
- Bremner-Bout M, Aartsma-Rus A, de Meijer EJ, Kaman WE, Janson AA, Vossen RH, et al. (2004). Targeted exon skipping in transgenic hDMD mice: a model for direct preclinical screening of human-specific antisense oligonucleotides. *Mol Ther* 10: 232–240.
- Fletcher S, Honeyman K, Fall AM, Harding PL, Johnson RD and Wilton SD (2006). Dystrophin expression in the mdx mouse after localized and systemic administration of a morpholino antisense oligonucleotide. *J Gene Med* 8: 202–216.
- Gebicki BL, Mann C, Fletcher S, and Wilton SD (2003). Morpholino antisense oligonucleotide induced dystrophin exon 23 skipping in mdx mouse muscle. *Hum Mol Genet* 12: 1801–1811.
- Aartsma-Rus A, Fokkema I, Verschuren I, Ginjaar I, van Deutekom J, van Ommeren GJ, et al. (2009). Theoretic applicability of antisense-mediated exon skipping for Duchenne muscular dystrophy mutations. *Hum Mutat* 30: 293–299.
- Aartsma-Rus A, van Deutekom J, Fokkema I, van Ommeren GJ and den Dunnen JT (2006). Entries in the Leiden Duchenne muscular dystrophy mutation database: an overview of mutation types and paradoxical cases that confirm the reading-frame rule. *Muscle Nerve* 34: 135–144.
- Prior TW, Bartolo C, Pearl DK, Papp AC, Snyder PJ, Sedra MS, et al. (1995). Spectrum of small mutations in the dystrophin coding region. *Am J Hum Genet* 57: 22–33.
- van Deutekom J, Janson AA, Ginjaar IB, Frankhuizen WS, Aartsma-Rus A, Bremner-Bout M, et al. (2007). Local dystrophin restoration with antisense oligonucleotide PRO051. *N Engl J Med* 357: 277–286.
- Kinali M, Archavala-Gomez Y, Feng L, Cirak S, Hunt D, Adkin C, et al. (2009). Local restoration of dystrophin expression with the morpholino oligomer AV1-658

- in Duchenne muscular dystrophy: a single-blind, placebo-controlled, dose-escalation, proof-of-concept study. *Lancet Neurol* **8**: 918–928.
25. Heiderman-van den Ende, AJ, Straatho, CS, Aartsma-Rus, A, den Dunnen, JT, Verbat, BM, Bakker, E et al. (2010). Becker muscular dystrophy patients with deletions around exon 51, a promising outlook for exon skipping therapy in Duchenne patients. *Neuromuscul Disord* **20**: 251–254.
 26. Hoffman, EP, Kunkel, LM, Angelini, C, Clarke, A, Johnson, M and Harris, JB (1989). Improved diagnosis of Becker muscular dystrophy by dystrophin testing. *Neurology* **39**: 1011–1017.
 27. Koenig, M and Kunkel, LM (1990). Detailed analysis of the repeat domain of dystrophin reveals four potential hinge segments that may confer flexibility. *J Biol Chem* **265**: 4560–4566.
 28. Carana, A, Friso, G, Tremolatersa, MR, Lanzillo, R, Vitale, DF, Santoro, L et al. (2005). Analysis of dystrophin gene deletions indicates that the hinge III region of the protein correlates with disease severity. *Ann Hum Genet* **69**(Pt 3): 253–259.
 29. Baumbach, LL, Chamberlain, JS, Ward, PA, Farwell, NJ and Caskey, CT (1989). Molecular and clinical correlations of deletions leading to Duchenne and Becker muscular dystrophies. *Neurology* **39**: 465–474.
 30. Gillard, EF, Chamberlain, JS, Murphy, EG, Duff, CL, Smith, B, Burghes, AH et al. (1989). Molecular and phenotypic analysis of patients with deletions within the deletion-rich region of the Duchenne muscular dystrophy (DMD) gene. *Am J Hum Genet* **45**: 507–520.
 31. Koenig, M, Beggs, AH, Moyer, M, Scherpf, S, Heinrich, K, Bettecken, T et al. (1989). The molecular basis for Duchenne versus Becker muscular dystrophy: correlation of severity with type of deletion. *Am J Hum Genet* **45**: 498–506.
 32. Corral-Vázquez, R, Arenas, D, Cisneros, B, Peñalosa, I, Kofman, S, Salamanca, F et al. (1993). Analysis of dystrophin gene deletions in patients from the Mexican population with Duchenne/Becker muscular dystrophy. *Arch Med Res* **24**: 1–6.
 33. Arai, E, Nakamura, K, Nakao, K, Kameya, S, Kobayashi, O, Nonaka, I et al. (1997). Targeted disruption of exon 52 in the mouse dystrophin gene induced muscle degeneration similar to that observed in Duchenne muscular dystrophy. *Biochem Biophys Res Commun* **238**: 492–497.
 34. Aartsma-Rus, A, Kamari, WE, Wei, R, den Dunnen, JT, van Ommen, CJ and van Deutekom, JC (2006). Exploring the frontiers of therapeutic exon skipping for Duchenne muscular dystrophy by double targeting within one or multiple exons. *Mol Ther* **14**: 401–407.
 35. De Angelis, FG, Standler, O, Berarducci, B, Toso, S, Galluzzi, G, Ricci, E et al. (2002). Chimeric snRNA molecules carrying antisense sequences against the splice junctions of exon 51 of the dystrophin pre-mRNA induce exon skipping and restoration of a dystrophin synthesis in Delta 48-50 DMD cells. *Proc Natl Acad Sci USA* **99**: 9456–9461.
 36. Aartsma-Rus, A, van Vliet, L, Hirschi, M, Janson, AA, Heemskerk, H, de Winter, CL et al. (2009). Guidelines for antisense oligonucleotide design and insight into splice-modulating mechanisms. *Mol Ther* **17**: 548–553.
 37. Adams, AM, Harding, PL, Iversen, PL, Coleman, C, Fletcher, S and Wilton, SD (2007). Antisense oligonucleotide induced exon skipping and the dystrophin gene transcript cocktails and chemistries. *BMC Mol Biol* **8**: 57.
 38. Banks, CB, Judge, LM, Allen, JM and Chamberlain, JS (2010). The polypyrrole site in hinge 2 influences the functional capacity of truncated dystrophins. *PLoS One* **6**: e1000958.
 39. Yoshimura, M, Sakamoto, M, Ikemoto, M, Mochizuki, Y, Yuasa, K, Miyagoe-Suzuki, Y et al. (2004). AAV vector-mediated microdystrophin expression in a relatively small percentage of human myofibers improved the mdx phenotype. *Mol Ther* **18**: 821–828.
 40. Wells, DJ, Wells, KE, Asante, EA, Turner, G, Sanada, Y, Campbell, KP et al. (1995). Expression of human full-length and mindy/dystrophin in transgenic mdx mice: implications for gene therapy of Duchenne muscular dystrophy. *Hum Mol Genet* **4**: 1245–1250.
 41. Mittpant, C, Adams, AM, Meloni, PL, Muntoni, F, Fletcher, S and Wilton, SD (2009). Rational design of antisense oligonucleotides to induce dystrophin exon skipping. *Mol Ther* **17**: 1418–1426.
 42. Wang, Q, Yin, H, Camilletti, P, Betts, C, Mouton, H, Lee, H et al. (2010). In vitro evaluation of novel antisense oligonucleotides is predictive of in vivo exon skipping activity for Duchenne muscular dystrophy. *J Gene Med* **12**: 354–364.
 43. Wu, B, Lu, P, Benrashed, E, Malik, S, Ashar, J, Doran, TJ et al. (2010). Dose-dependent restoration of dystrophin expression in cardiac muscle of dystrophic mice by systemically delivered morpholino. *Gene Ther* **17**: 132–140.
 44. Reagan-Shaw, S, Nihal, M and Ahmad, N (2008). Dose translation from animal to human studies revisited. *FASEB J* **22**: 659–661.
 45. de Lateur, BJ and Giacconi, RM (1979). Effect on maximal strength of submaximal exercise in Duchenne muscular dystrophy. *Am J Phys Med* **58**: 26–36.
 46. Shivers, RR and Atkinson, BG (1984). The dystrophic murine skeletal muscle cell plasma membrane is structurally intact but "leaky" to creatine phosphokinase. A freeze-fracture analysis. *Am J Pathol* **116**: 482–496.
 47. Heemskerk, H, de Winter, C, van Kulk, P, Heuvelmans, N, Sabatelli, P, Rimessi, P et al. (2010). Preclinical PK and PD studies on 2'-O-methyl-phosphorothioate RNA antisense oligonucleotides in the mdx mouse model. *Mol Ther* **18**: 1210–1217.
 48. Porter, JD, Guo, W, Merriam, AP, Khanna, S, Cheng, G, Zhou, X et al. (2003). Persistent over-expression of specific CC class chemokines correlates with macrophage and T-cell recruitment in mdx skeletal muscle. *Neuromuscul Disord* **13**: 223–235.
 49. Demoule, A, Dvaghghi, M, Danelou, G, Gvozdic, D, Larkin, C, Bao, W et al. (2005). Expression and regulation of CC class chemokines in the dystrophic (mdx) diaphragm. *Am J Respir Cell Mol Biol* **33**: 178–185.
 50. Liu, QJ, Rabinowitz, A, Chen, YJ, Yokota, T, Yin, H, Alter, J et al. (2005). Systemic delivery of antisense oligonucleotide restores dystrophin expression in body-wide skeletal muscles. *Proc Natl Acad Sci USA* **102**: 198–203.
 51. Spitali, P, Heemskerk, H, Vossen, RH, Ferlini, A, den Dunnen, JT, 't Hoen, PA et al. (2010). Accurate quantification of dystrophin mRNA and exon skipping levels in Duchenne Muscular Dystrophy. *Lab Invest* (epub ahead of print).

Post-translational Maturation of Dystroglycan Is Necessary for Pikachurin Binding and Ribbon Synaptic Localization^{*[5]}

Received for publication, February 20, 2010, and in revised form, July 23, 2010. Published, JBC Papers in Press, August 3, 2010, DOI 10.1074/jbc.M110.116343

Motoi Kanagawa¹, Yoshihiro Omori², Shigeru Sato³, Kazuhiro Kobayashi¹, Yuko Miyagoe-Suzuki¹, Shin'ichi Takeda⁴, Tamao Endo¹, Takahisa Furukawa⁵, and Tatsushi Toda¹

From the ¹Division of Neurology/Molecular Brain Science, Kobe University Graduate School of Medicine, Kobe 650-0017, the ²Department of Developmental Biology, Osaka Bioscience Institute, Japan Science and Technology Agency, Core Research for Evolutional Science and Technology, Suita 565-0874, the ³Department of Molecular Therapy, National Institute of Neuroscience, National Center of Neurology and Psychiatry, Kodaira 187-8502, and ⁴Molecular Glycobiology, Tokyo Metropolitan Institute of Gerontology, Tokyo 173-0015, Japan

Pikachurin, the most recently identified ligand of dystroglycan, plays a crucial role in the formation of the photoreceptor ribbon synapse. It is known that glycosylation of dystroglycan is necessary for its ligand binding activity, and hypoglycosylation is associated with a group of muscular dystrophies that often involve eye abnormalities. Because little is known about the interaction between pikachurin and dystroglycan and its impact on molecular pathogenesis, here we characterize the interaction using deletion constructs and mouse models of muscular dystrophies with glycosylation defects (*Large*^{mvd} and *POMGnT1*-deficient mice). Pikachurin-dystroglycan binding is calcium-dependent and relatively less sensitive to inhibition by heparin and high NaCl concentration, as compared with other dystroglycan ligand proteins. Using deletion constructs of the laminin globular domains in the pikachurin C terminus, we show that a certain steric structure formed by the second and the third laminin globular domains is necessary for the pikachurin-dystroglycan interaction. Binding assays using dystroglycan deletion constructs and tissue samples from *Large*-deficient (*Large*^{mvd}) mice show that *Large*-dependent modification of dystroglycan is necessary for pikachurin binding. In addition, the ability of pikachurin to bind to dystroglycan prepared from *POMGnT1*-deficient mice is severely reduced, suggesting that modification of the GlcNAc- β 1,2-branch on *O*-mannose is also necessary for the interaction. Immunofluorescence analysis reveals a disruption of pikachurin localization in the photoreceptor ribbon synapse of these model animals. Together, our data demonstrate that post-translational modification on *O*-mannose, which is mediated by *Large* and *POMGnT1*, is essential for pikachurin binding and proper localization, and suggest that their disruption underlies the molecular pathogenesis of eye abnormalities in a group of muscular dystrophies.

Dystroglycan (DG)², a cell surface receptor for several extracellular matrix proteins, plays important roles in various tissues (1–7). DG consists of an extracellular, heavily glycosylated α subunit (α -DG) and a transmembrane β subunit (β -DG). α -DG and β -DG are encoded by a single gene and post-translationally cleaved to generate the two subunits. α -DG is a receptor for extracellular proteins such as laminin-111, laminin-211, agrin, perlecan, and neurexin. β -DG binds to α -DG in the extracellular space, anchoring α -DG at the cell surface. Inside the cell, β -DG binds to dystrophin, which in turn is linked to the actin cytoskeleton. Thus, α/β -DG functions as a molecular axis, connecting the extracellular matrix with the cytoskeleton across the plasma membrane.

DG ligand proteins commonly contain laminin globular (LG) domains, which mediate binding to α -DG. *O*-Mannosylation of α -DG is required for its interaction with ligands; however, the precise ligand-binding sites and epitope are not known. A unique *O*-mannosyl tetrasaccharide (Neu5Ac- α 2,3-Gal- β 1,4-GlcNAc- β 1,2-Man) was first identified on peripheral nerve α -DG (8). The initial Man transfer to Ser/Thr residues on the α -DG peptide backbone is catalyzed by the POMT1-POMT2 complex (9). Both *POMT1* and *POMT2* were originally identified as responsible genes in Walker-Warburg syndrome (10, 11). *POMGnT1*, a causative gene for muscle-eye-brain disease, encodes a glycosyltransferase that transfers GlcNAc to *O*-Man on α -DG (12). Because mutations in these enzymes cause abnormal glycosylation of α -DG and reduce its ligand binding activity, it is recognized that the GlcNAc- β 1,2-branch on *O*-Man is essential to α -DG function as a matrix receptor.

Additional proteins, including fukutin, FKRP, and LARGE, are also involved in synthesizing the glycans on α -DG that are required for ligand binding activity. Recently, a GalNAc- β 1,3-GlcNAc- β 1,4-branch and a phosphodiester-linked modification on *O*-Man were identified (13). α -DG from cells with mutations in *fukutin* or *Large* shows defective post-phosphoryl modification on *O*-Man, suggesting that this phosphoryl branch serves a laminin-binding moiety. *fukutin* was originally identified as the responsible gene for Fukuyama-type congenital muscular dystrophy (14), and the *fukutin* homologue *FKRP* was identified through sequence homology (15). Mutation of

^{*} This work was supported by Ministry of Health, Labor, and Welfare of Japan Intramural Research Grant for Neurological and Psychiatric Disorders of the National Center of Neurology and Psychiatry 208-13, Research on Psychiatric and Neurological Diseases and Mental Health Grant H20-016 (to T. T.), Japan Society for the Promotion of Science Grant-in-aid for Young Scientists (B) 21790318, and Grant-in-aid for Scientific Research on Priority Areas 20056020 (to M. K.).

^[5] The on-line version of this article (available at <http://www.jbc.org>) contains supplemental Figs. 1–5.

¹ To whom correspondence should be addressed: 7-5-1 Kusunoki-chou, Chuo-ku, Kobe 650-0017, Japan. Tel.: 81-78-382-6287; Fax: 81-78-382-6288; E-mail: toda@med.kobe-u.ac.jp.

² The abbreviations used are: DG, dystroglycan; ERG, electroretinogram; LG, laminin globular.

LARGE, a putative glycosyltransferase, generates spontaneous muscular dystrophy in the *Large^{msd}* mouse model (16). A unique feature of LARGE is that its overexpression produces a hyperglycosylated α -DG that shows increased laminin binding activity, even in cells with genetic defects in the α -DG glycosylation pathway (17).

Mutations in each of these genes (*POMT1*, *POMT2*, *POMGnT1*, *fukutin*, *FKRP*, and *LARGE*) have been identified in congenital and limb-girdle forms of muscular dystrophy (18). A common characteristic of patients who have such mutations is abnormal glycosylation of α -DG; thus, these conditions are collectively referred to as dystroglycanopathies. The clinical spectrum of dystroglycanopathy is broad, ranging from severe congenital onset associated with structural brain malformations to a milder congenital variant with no brain involvement and to limb-girdle muscular dystrophy type 2 variants with childhood or adult onset (18, 19). Eye abnormalities are often associated with more severe dystroglycanopathy, such as Walker-Warburg syndrome and muscle-eye-brain disease (20). The ophthalmologic phenotype of muscular dystrophy is also known for Duchenne/Becker muscular dystrophy, which is caused by dystrophin mutations. Most patients with Duchenne/Becker muscular dystrophy have evidence of abnormal electroretinograms (ERG) (21).

Pikachurin, the most recently identified DG ligand protein, is localized in the synaptic cleft in the photoreceptor ribbon synapse (22). Like other DG ligands, pikachurin contains LG domains in its C-terminal region. Pikachurin-null mutant mice show improper apposition of the bipolar cell dendritic tips to the photoreceptor ribbon synapses, resulting in altered synaptic signal transmission and visual function. Similar retinal electrophysiological abnormalities, such as attenuated or delayed b-wave, have been observed in *Large^{msd}* (23) and *POMGnT1*-deficient mice (24). These studies imply a functional relationship between pikachurin and DG glycosylation in the retinal ribbon synapse.

In this study, we have biochemically characterized the interaction between pikachurin and α -DG. We have found that both GlcNAc- β 1,2-branch and LARGE-dependent modification on *O*-Man are necessary for the pikachurin-DG interaction. Furthermore, in dystroglycanopathy model animals, pikachurin localization in the retinal synaptic outer plexiform layer is severely disrupted. These data demonstrate that post-translational maturation of DG is essential for pikachurin binding and proper localization, providing a possible molecular explanation for the retinal electrophysiological abnormalities observed in dystroglycanopathy patients.

EXPERIMENTAL PROCEDURES

Vector Construction and Protein Expression—Construction of recombinant mouse pikachurin LG domains (PikaLG; residues 391–1017) has been described previously (22). Single or tandem LG domains were constructed using PCR, with a full-length PikaLG expression vector as the template cDNA. Primers used were as follows: LG1(391–627), PikaKpn (CTTGGTACCGAGC-TCGGATC) and E627r (TTCTCGAGCCTCCAGGGGCCAGG-GTGTG); LG2(542–838), G542f (TTGGTACCGAGCTCGGA-TCTGGGAAGAAGATTGACATGAG) and P838r (TTCTCG-

AGCTGGGATCTCGATGGCTTCTA); LG3(799–1017), D766f (TTGGTACCGAGCTCGGATCTGACCGGACCATCCATGTGAAG) and PikaR (GCAACTAGAAGGCACAGTCG); LG1-2(391–883), PikaKpn and P838r; and LG2-3(542–1017), G542f and PikaR. PCR products were digested with KpnI/XhoI and inserted into the KpnI/XhoI sites of the pSecTag2 vector (Invitrogen).

Recombinant mouse α -DG fused to an Fc tag (DGFC) also has been described previously (22). Deletion mutants were constructed using PCR, with the wild-type DGFC vector as the template cDNA. Primers used were as follows: DG-N(1-313), pCAGf (AAGAATTCGCGCCACCATGAGG) and DGFC313r (AATCTAGATTTGGGGAGAGTGGGCTTCTT); DGAN(1–28 plus 315–651), pCAGf and DGFC28r (GGCCTGAGCCACAGCCACAGACAGGAGGAG); and DGFC315f (ACACCTACACCTGTACTGCC) and Fexxon2r (TCCC-CAGAGAGTTCAGGTTGC); DGAC(1–483), pCAGf and DGFC483r (AATCTAGAAGGAATTTGTCAGTGTGG-GCG); DG^{half}(1–407), pCAGf and DGFC407r (AATCTAGAA-CTGGTGGTAGTACGGATTCC). PCR products were digested with EcoRI/XbaI and inserted into the EcoRI/XbaI sites of the wild-type DGFC expression vector.

PikaLG and DGFC constructs were expressed in HEK293 cells (22). For preparation of PikaLG-containing cell lysates, transfected cells were solubilized in lysis buffer (1% Nonidet P-40, 10% glycerol, 50 mM Tris-HCl, pH 7.5, 150 mM NaCl, and a protease inhibitor mixture). The samples were centrifuged at 15,000 rpm for 10 min at 4 °C, and the supernatants were used for binding assays.

DGFC proteins were secreted into the cell culture media and recovered with protein A or protein G beads. For the solid-phase binding assays, DGFC proteins were eluted with 0.1 M glycine HCl, pH 2.5, and then neutralized to a final concentration of 0.2 M Tris-HCl, pH 8.0. Protein concentrations of the cell lysates and the DGFC proteins were determined using Lowry's method (Bio-Rad) with BSA as a standard.

Antibodies—Antibodies used for Western blots and immunofluorescence were as follows: mouse monoclonal antibody 8D5 against β -DG (Novacastra); rabbit polyclonal antibody against β -DG (Santa Cruz Biotechnology); mouse monoclonal antibody IIH6 against α -DG (Upstate); goat polyclonal antibody against the α -DG C-terminal domain (AP-074G-C) (25); and rabbit polyclonal antibodies against pikachurin (22).

Animals—C57BL/6 mice were obtained from Japan SLC, Inc., and *Large^{msd}* mice were obtained from The Jackson Laboratory. Generation of *POMGnT1*-deficient mice has been described previously (26). Mice were maintained in accordance with the animal care guidelines of Osaka University and Kobe University.

Pikachurin Binding Assay—For the DGFC pull-down assay, secreted DGFC proteins were recovered from conditioned media using protein A beads (10 μ l). DGFC-protein A bead complexes were washed with TBS (50 mM Tris-HCl, pH 7.4, and 150 mM NaCl) and incubated with cell lysates containing PikaLG proteins in the presence of 2 mM CaCl₂ overnight at 4 °C. After five washes with washing buffer (0.1% Nonidet P-40, 50 mM Tris-HCl, pH 7.5, 150 mM NaCl, 2 mM CaCl₂), bound materials were eluted with SDS-sample buffer. Bound materials

Pikachurin-Dystroglycan Interaction

were analyzed by Western blotting using anti-His or anti-Myc tag antibodies and the anti-Fc antibody.

For the solid-phase binding assays, DGFc preparations (2.5 μg) were coated on ELISA microplates (Costar) for 16 h at 4 °C. Plates were washed in TBS and blocked for 2 h with 3% BSA in TBS. PikaLG-containing cell lysates (8 μg) in binding buffer (3% BSA, 1% Nonidet P-40, 2 mM CaCl_2 in TBS) were applied and incubated overnight at 4 °C. Wells were washed with TBS containing 1% BSA, 0.1% Nonidet P-40, and 1 mM CaCl_2 for three times and incubated for 30 min with 1:1,000 anti-Myc (Santa Cruz Biotechnology) followed by anti-rabbit HRP. Plates were developed with *o*-phenylenediamine dihydrochloride and H_2O_2 . Reactions were stopped with 2 N H_2SO_4 , and values were obtained using a microplate reader. BSA-coated wells were used to subtract nonspecific binding. For Ca^{2+} concentration dependence, the data were fit to the equation $A = B_{\text{max}}x/(K_d + x)$, where K_d is the concentration required to reach half-maximal binding; A is absorbance, and B_{max} is maximal binding. All data were obtained as the means of triplicate measurements. Each experiment was repeated more than three times, and data are represented as the average of at least three independent experiments with standard deviations. Statistical analysis was performed with a two-tailed paired *t* test (GraphPad prism). A *p* value of <0.05 was considered to be significant.

For binding assays with PikaLG deletion proteins, we confirmed protein expression via Western blot analysis. Cell lysates containing comparable amounts of each LG deletion protein were adjusted by adding mock-transfected cell lysate to achieve a normalized total protein concentration across reaction mixtures.

DG Enrichment and Immunoprecipitation—For solid-phase binding assays with brain DG, mouse brain tissue (200 mg) was homogenized in 1.8 ml of TBS with a proteinase inhibitor mixture and then solubilized with 1% Triton X-100. Samples were centrifuged at 15,000 rpm for 10 min, and the supernatants were incubated with 50 μl of wheat germ agglutinin-agarose beads (Vector Laboratories) overnight at 4 °C. The beads were washed three times in 1 ml of TBS containing 0.1% Triton X-100 and then eluted with 250 μl of TBS containing 0.1% Triton X-100 and 200 mM *N*-acetylglucosamine. The presence of comparable amounts of DG protein in each elution was confirmed via Western blot analysis with DG antibodies, as described above.

To immunoprecipitate α -DG from mouse tissues, mouse brains or eyes were homogenized in TBS with a proteinase inhibitor mixture and then solubilized with 1% Triton X-100. Samples were centrifuged at 15,000 rpm for 10 min, and then the supernatants were incubated with or without anti- α -DG core protein (25). α -DG was immunoprecipitated using protein G beads. The α -DG-protein G beads were washed with TBS containing 0.1% Triton X-100 three times and then tested for binding with PikaLG, as described above.

Heparin Affinity Beads—PikaLG-containing cell lysates were incubated with the heparin beads (Sigma) overnight at 4 °C. After three washes with TBS containing 0.1% Nonidet P-40, bound materials were eluted with SDS-sample buffer.

Immunofluorescent Staining—Mouse eye cups were fixed in 4% paraformaldehyde/phosphate-buffered saline (PBS) for 30

min. Samples were cryoprotected, embedded, frozen, and sectioned 20 μm thick. Slides were incubated with blocking solution (5% normal goat serum and 0.5% Triton X-100 in PBS) for 1 h. Sections were incubated with primary antibodies at room temperature for 4 h, washed with PBS for 10 min, and incubated with secondary antibodies for 2 h. The sections were covered with Gelvatol after rinsing with 0.02% Triton X-100 in PBS.

Quantitative Real Time PCR Analysis—Total RNA (1 μg) from the mouse retina was isolated using TRIzol reagent (Invitrogen) and converted to cDNA using Superscript II RTase (Invitrogen). Quantitative real time PCR was performed using SYBR Green ER qPCR Super MIX (Invitrogen) and the Thermal Cycler Dice Real Time System single MRQ TP870 (Takara) according to the manufacturer's instructions. Quantification was performed using Thermal Cycler Dice Real Time System software version 2.0 (Takara). Primers used in gene amplification were as follows: amplification of the pikachurin gene, Pikachurin-F, GGAAGATTACAGTGGATGACTACG, and Pikachurin-R, GTGTGCGAGCGGATTTCTTCATTC; amplification of β -actin gene, actin-F, CGTGGGTGACATCAAGAGAA, and actin-R, TGGATGCCACAGGATTCAT.

RESULTS

Properties of the Pikachurin-Dystroglycan Interaction—To analyze binding between pikachurin and α -DG, we used recombinant pikachurin LG domains with a myc-His tandem tag (PikaLG) and α -DG fused to an Fc tag (DGFc) (Fig. 1A) (22). Previous data suggest that the pikachurin-DG interaction requires divalent cations (22). To further characterize this requirement, we analyzed PikaLG-DGFC binding in the presence of Ca^{2+} , Mg^{2+} , or Mn^{2+} using a pull-down assay (Fig. 1B). Ca^{2+} produced the strongest binding, whereas Mn^{2+} gave only faint binding, and no binding was observed with Mg^{2+} alone. To evaluate PikaLG-DGFC binding quantitatively, we developed a solid-phase binding assay. DGFc was immobilized on microplates, and cell lysates containing PikaLG were applied for binding. Signals representing binding of PikaLG to DGFc were detected, whereas no detectable signal was obtained from mock-transfected cell lysates (supplemental Fig. 1). Immobilized Fc protein showed no difference in signal intensity between PikaLG-containing and mock-transfected cell lysates, confirming the lack of specific interactions through the Fc portion (supplemental Fig. 1). We concluded that the solid-phase binding assay is sufficient to quantitatively detect PikaLG-DGFC interactions. The solid-phase binding assays showed results comparable with the pull-down assays. We observed a reduction in binding of around 70% in the presence of Mn^{2+} and a strong reduction in the presence of Mg^{2+} , similar to that seen in the presence of EDTA for chelation of divalent cations (Fig. 1C). The solid-phase binding assays in various Ca^{2+} concentrations established that the concentration required for half-maximal binding is $\sim 80 \mu\text{M}$ (Fig. 1D). It has been reported that heparin or a high NaCl concentration (0.5 M) inhibits binding of laminin-111 and agrin to α -DG (27, 28). We examined the effects of heparin and NaCl on PikaLG-DGFC binding. The results showed that PikaLG-DGFC binding was inhibited slightly at 0.5 M NaCl ($\sim 80\%$ binding), and the inhibitory effect

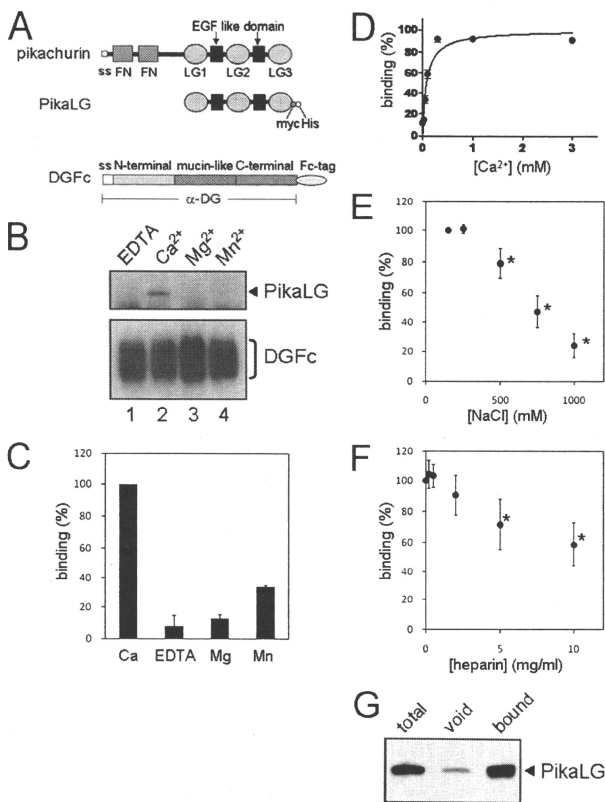


FIGURE 1. Biochemical characterization of pikachurin-dystroglycan interaction. *A*, Schematic representation of recombinant pikachurin and α -DG. Pikachurin contains a signal sequence (ss), two fibronectin 3 (FN) domains, three laminin globular (LG) domains, and two calcium-binding EGF-like (EGF-like) domains. Recombinant pikachurin LG domains (PikaLG) contain amino acid residues 391–1071 and a tandem myc-His tag at the C terminus. α -DG contains the signal sequence (ss), N-terminal, mucin-like, and C-terminal domains. Recombinant α -DG (DGFC) has an Fc tag at the C terminus. *B*, Divalent cation is necessary for pikachurin-dystroglycan interaction. PikaLG binding to DGFC-protein A beads was tested in the presence of 2 mM EDTA (lane 1) and 2 mM each of Ca^{2+} (lane 2), Mg^{2+} (lane 3), or Mn^{2+} (lane 4). Bound PikaLG was detected by Western blotting with an anti-His tag antibody (upper panel, indicated by PikaLG). Comparable amounts of DGFC proteins on protein A beads were confirmed by staining with an anti-Fc antibody (lower panel, indicated by DGFC). *C*, Quantitative solid-phase binding assays for divalent cation dependence. PikaLG binding to immobilized DGFC was tested in the presence of 2 mM EDTA and 2 mM each of Ca^{2+} , Mg^{2+} , or Mn^{2+} . Binding in the presence of Ca^{2+} was set as 100%. Data shown are the average of three independent experiments with standard deviations. *D*, Ca^{2+} -dependent binding of pikachurin to dystroglycan. PikaLG binding to DGFC was tested in various Ca^{2+} concentrations by solid-phase binding assays. The binding data were fit to the equation $Y = B_{\text{max}}x/(K_d + x)$, where K_d is the concentration required to reach half-maximal binding, and B_{max} is maximal binding. Maximal binding was set as 100%. $K_d = 78 \pm 15 \mu\text{M}$. Data shown are the average of four independent experiments with standard deviations. *E* and *F*, effects of NaCl (*E*) and heparin (*F*) on the pikachurin-dystroglycan interaction. PikaLG binding to DGFC was tested in various NaCl or heparin concentrations by solid-phase binding assays. Binding in the presence of 150 mM NaCl (*E*) or in the absence of heparin (*F*) was set as 100%. Data shown are the average of four (*E*) and six (*F*) independent experiments with standard deviations. *G*, Binding of pikachurin LG domains to heparin. Lysates from PikaLG-expressing cells were incubated with heparin affinity beads. Total lysate sample (total, lane 1), flow-through (void, lane 2), and bound (bound, lane 3) fractions were analyzed by Western blotting with an antibody to anti-Myc tag.

increased with higher concentrations of NaCl (Fig. 1E). No significant inhibitory effect was detected with heparin at 2 mg/ml (Fig. 1F), which is a sufficient concentration to completely inhibit α -DG binding to laminin-111 or agrin (28, 29). At 10 mg/ml heparin, PikaLG-DGFC binding was reduced to 60% (Fig. 1F). We confirmed that these conditions (0.5 M NaCl and 2 mg/ml heparin) do inhibit laminin-111 binding to DGFC (data not shown). To examine whether PikaLG has heparin binding capacity, we exposed lysates prepared from PikaLG-expressing cells to heparin affinity beads (Fig. 1G). Binding of PikaLG to heparin affinity beads was positive, indicating that PikaLG contains a heparin-binding site.

Dissection of Domains Necessary for Pikachurin-Dystroglycan Interaction—All known DG ligand proteins (laminin-111, laminin-211, agrin, perlecan, and neuexin) contain LG domains, through which they bind to α -DG. Pikachurin contains three LG domains in its C terminus. To examine which LG domain serves as the α -DG-binding site, we constructed single or tandem LG domains (Fig. 2A) and examined DGFC binding to each construct. We confirmed expression of all constructs in cells and then tested cell lysates containing comparable amounts of each LG protein for binding to DGFC (Fig. 2B). We found that the LG2-LG3 tandem construct binds to DGFC at a level similar to that of the full-length construct (Fig. 2B, right panel, lanes 5 and 6). Binding of other constructs to DGFC was minimal or undetectable. Solid-phase binding assays also confirmed that LG2-3 bound to DGFC, whereas the other deletion constructs did not (Fig. 2C). When PikaLG deletion constructs were subjected to SDS gel electrophoresis without heat denaturing, the constructs containing LG1 domains appeared at higher molecular weights than observed with heat denaturing (Fig. 2D). This result indicates that pikachurin forms oligomeric structures. Al-

Pikachurin-Dystroglycan Interaction

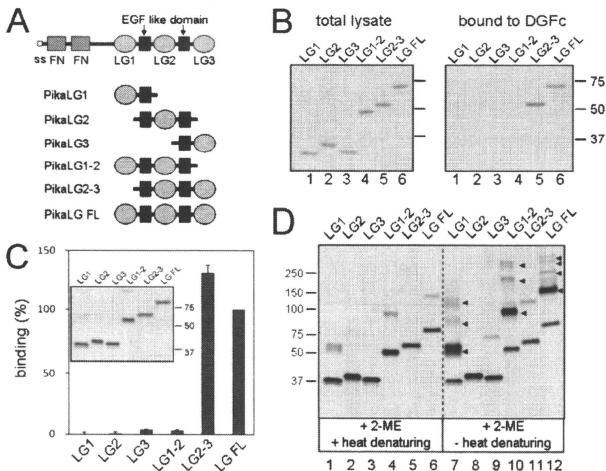


FIGURE 2. Dissection of the dystroglycan binding region in pikachurin. A, schematic representation of pikachurin deletion mutant proteins. All constructs contain a tandem myc-His tag at the C terminus. ss, signal sequence. B, binding of pikachurin deletion constructs to dystroglycan. Each deletion construct was expressed in HEK293 cells, and cell lysates were subjected to the DGFc binding assay. PikaLG in the reaction mixture (left panel) and PikaLG bound to DGFc-protein G-beads (right panel) were analyzed by Western blotting with an anti-Myc tag antibody. C, solid-phase binding assays for pikachurin deletion constructs. Cell lysates containing an equal amount of each deletion construct were tested for DGFc binding. Binding of full-length DGFc was set as 100%. Data shown are the average of four independent experiments with standard deviations. Inset, Western blot analysis to confirm the amount of each LG protein used in the binding assays. D, oligomer Western blot analysis of pikachurin. Cell lysates containing comparable amounts of each construct were dissolved in SDS sample buffer containing 2-mercaptoethanol (2-ME) and then subjected to SDS-PAGE with (+2-ME, +heat denaturing) or without (+2-ME, -heat denaturing) heat denaturing (95 °C, 5 min). Constructs containing LG1 (LG1, LG1-2, and LG FL) showed several higher molecular weight bands (arrowheads), which might indicate oligomeric structure formation by pikachurin.

though we observed no positive effect of the LG1 domain on PikaLG-DGFC binding, LG1-mediated oligomerization might play a physiological role in a more native situation. Overall, our results indicate that a certain steric structure formed by the LG2 and the LG3 domains is necessary for the pikachurin-DG interaction.

LARGE plays a crucial role in the DG modification process (17, 30). For LARGE-dependent modification of α -DG, two distinct domains of α -DG, the N-terminal domain and the first half of the mucin-like domain, are necessary. The N-terminal domain of α -DG is recognized by LARGE during post-translational maturation of DG and then proteolytically removed. The first half of the mucin-like domain of α -DG is modified with certain glycans necessary for acquiring ligand binding activity (30). To investigate whether these domains of α -DG are required for pikachurin binding, we used several DGFC deletion constructs (Fig. 3A). DG-N, which contains only the N-terminal domain, did not bind to PikaLG (Fig. 3B, lane 2). DG Δ N, which lacks the N-terminal domain, also failed to bind to PikaLG, even though it contains the entire mucin-like domain (Fig. 3B, lane 3). Co-expression with LARGE enhanced PikaLG binding to full-length DGFC (DG-wt) (Fig. 3B, lanes 4 and 5).

Using deletion constructs lacking the C-terminal domain (DGAC) or containing the N-terminal domain plus the first half of the mucin-like domain (and DG^{half}), we showed that pikachurin-binding domains are located within the first half of the mucin-like domain (Fig. 3C). We examined binding of laminin-111 to these constructs using an overlay assay and confirmed that PikaLG binds to the same constructs that are able to capture laminin-111 (Fig. 3, B and C, bottom panels).

Disruption of Pikachurin Binding and Localization in Dystroglycanopathy Animals—We investigated various aspects of the pikachurin-DG interaction in dystroglycanopathy model animals. First, we used *POMGnT1*-deficient mice to investigate whether the GlcNAc- β , 2-branch on O-Man is necessary for pikachurin binding. Endogenous α -DG was immunoprecipitated from brain extracts of *POMGnT1*-deficient and littermate heterozygous mice using antibodies that recognize the α -DG core protein (AP-G074). Precipitates were then incubated with lysates prepared from PikaLG-expressing cells (Fig. 4A). Western blot analysis of the immunoprecipitated materials confirmed that α -DG from the

POMGnT1-deficient samples was hypoglycosylated, as evidenced by reduced molecular size. Whereas PikaLG bound to control α -DG of normal molecular size, the PikaLG- α -DG interaction was dramatically reduced in *POMGnT1*-deficient mice.

Next, we examined whether native α -DG from *Large*^{myd} (myd) mice binds to pikachurin. Endogenous α -DG was immunoprecipitated from brains of myd or control heterozygous mice and then tested for pikachurin binding (Fig. 4B). We observed PikaLG binding to control α -DG with normal molecular size but not to hypoglycosylated α -DG from the myd mouse brain.

We also examined the PikaLG binding to native α -DG prepared from these mutant mice brains by solid-phase assays. Although binding signals obtained from the native DG preparations were generally weaker than those of DGFC, Ca²⁺-sensitive binding was detected in control heterozygous samples (Fig. 4C). However, no significant binding was detected in mutant samples. These data indicate that the pikachurin-DG interaction is disrupted in dystroglycanopathy animals.

We also examined pikachurin expression and localization in the ribbon synapses of *POMGnT1*-deficient and myd mice.